A BIO-ADJUVANT COMBINATION APPROACH FOR THE CHEMOPREVENTION OF ORAL CANCER: PRECLINICAL TRIALS

by

Katelyn Ann DiBernardo Bothwell

February 2015

A thesis submitted to the
Faculty of the Graduate School of
the University at Buffalo, State University of New York
in partial fulfillment of the requirements for the

degree of

Master of Science

Natural Sciences Interdisciplinary Program
Roswell Park

ProQuest LLC.
789 East Eisenhower Parkway
P.O. Box 1346
Ann Arbor, MI 48106 - 1346

ACKNOWLEDGEMENTS

I would like to express my deep gratitude to my PI/mentor, Dr. Mukund Seshadri, for his continual guidance, support, and the opportunity to be a member of his laboratory. I would also like to thank my committee member, Dr. Pamela Hershberger, for her guidance and input on multiple facets of my thesis project. I must also thank the members of the Seshadri lab, Margaret Folaron and Laurie Rich. Margaret helped me with numerous aspects of my research, and I cannot thank her enough for everything she has done for me. Margaret's and Laurie's assistance, unconditional support, and guidance will be forever appreciated. I would also like to thank the members of the Hershberger lab who have assisted me in aspects of my studies, in particular, Tatiana Shaurova. I would like to acknowledge the members of the Small Animal Bio-Imaging Resource, Steven Turowski and Dr. Joseph Spernyak, members of the Pathology Resource Network, and the Mouse Tumor Model Resource at RPCI for their technical assistance. I would also like to acknowledge and thank the Roswell Park Alliance Foundation for funding this research. My experience in the Seshadri lab at Roswell Park has been more fulfilling and influential than I could have hoped for, and I am extremely appreciative of everyone who has made my experience and project possible. I would finally like to thank my family for their unconditional support, love, and patience. They have been my foundation and encouragement throughout my life, and I am deeply grateful for everything they have done and continue to do for me.

CONTENTS

FIGURE INDEX

ABSTRACT

Purpose: Epidermal growth factor receptor (EGFR) activation is an early event in head and neck carcinogenesis. As a result, targeting EGFR has become an attractive strategy for chemoprevention. We examined the impact of using calcitriol, the active metabolite of vitamin D, as a bio-adjuvant in combination with the EGFR inhibitor, erlotinib, in the prevention of oral cancer.

Methods: Experimental studies were conducted in the 4-nitroquinoline-1-oxide (4NQO) oral carcinogenesis model to study the chemopreventive efficacy of calcitriol and erlotinib treatment, as single agents and in combination. Imaging results were correlated with histology and immunoblotting analyses to assess the impact of the combination regimen on oral carcinogenesis. Incidence of tumor development and evidence of disease progression were utilized as measures of response. Body weight measurements were acquired throughout the study as an assessment of systemic toxicity and echocardiography was performed to assess the effect of combination treatment on cardiac function.

Results: All control animals showed visible lesions on MRI examination at 26 weeks. Combination treatment was well tolerated and was not associated with any toxicity. MRI revealed a reduction in tumor incidence and tumor volume following treatment with erlotinib alone and in combination. Histopathologic evaluation revealed a reduction in the degree of dysplasia with combination treatment. Immunoblot analysis of whole tongue extracts revealed decreased expression of phospho-EGFR and phospho-Akt with the combination treatment.

Conclusion: These results demonstrate the potential of combining calcitriol with erlotinib in the chemoprevention of head and neck cancer. Further investigation into the optimal schedule and dosing of this combination strategy is necessary. In addition, future studies examining the use of less calcemic vitamin D_3 analogues and dietary vitamin D against this disease is warranted.

CHAPTER 1. BACKGROUND

1.1. Head and Neck Cancer

Head and neck squamous cell carcinoma (HNSCC) is the sixth most common cancer and accounts for approximately 350,000 yearly deaths worldwide (1). Malignancies of the head and neck are primarily epithelial-based and can constitute tumors that originate in multiple anatomical sites including the oral cavity, oropharynx, larynx and hypopharynx. Oral cancer is the most commonly diagnosed form of head and neck cancer and is often preceded by precursor lesions such as leukoplakia, erythroplakia, or erythroleukoplakia (2, 3). In addition to having anatomical heterogeneity, HNSCC is also characterized by its molecular heterogeneity due to 'field cancerization'. Field cancerization refers to the presence of one or more mucosal areas having epithelial cells that display cancer-associated genetic or epigenetic alterations (3). This unique biology contributes to tumor recurrence and/or the growth of a second primary tumor in a neighboring field (3). Two of the most common risk factors for oral and head and neck cancers include tobacco use and alcohol consumption, which have been shown to have a synergistic effect when used together (4, 5). HNSCC patients often have a poor prognosis due to the late stage in which the disease is diagnosed; less than 50% of patients diagnosed in advanced stages survive for 5 years, during which overall quality of life post-treatment is drastically reduced (6, 7).

Treatment of HNSCC patients differs based upon the stage of disease at diagnosis. Early-stage malignancies are treated primarily with either surgery or radiation therapy, while later stage tumors are often treated with both surgery and radiation (8, 9). Within the past ten years, there has been an increase in treatment involving combined chemoradiation and surgery (3). Although these treatment strategies exhibit moderate efficacy among HNSCC patients, these strategies also are non-selective and can cause damage to normal tissue, as well as have systemic toxic effects

(6). There is a need for safe and effective treatment strategies for the head and neck patient population. More recently, molecular-targeted drugs have been used for treatment of HNSCC that have enabled organ preservation (3, 9-11).

1.2. Targeting the Epidermal Growth Factor in HNSCC

The epidermal growth factor receptor (EGFR) is the only proven molecular target for treatment of HNSCC (12, 13). The epidermal growth factor receptor is a cell-surface glycoprotein that consists of three domains, an extra-cellular ligand-binding domain, a hydrophobic transmembrane domain, and an intracellular tyrosine kinase domain (14). Activation of the EGFR results in activation of intracellular signaling pathways that can lead to inhibition of apoptosis, activation of cell proliferation and angiogenesis, as well as an increase in the potential for metastasis (15). EGFR is overexpressed in up to 80-90% of HNSCC cases and level of expression can be an indication of prognosis (16). High expression of EGFR is associated with increased tumor size, decreased radiation sensitivity and increased risk of recurrence, collectively resulting in decreased overall survival (17-21). Two main pharmacologic approaches exist to inhibit the EGFR. The first approach, and currently the most clinically successful, is use of a monoclonal antibody (mAb). Monoclonal antibodies specifically inhibit the extracellular-binding domain, preventing endogenous ligands, such as, epidermal growth factor (EGF) and transforming growth factor alpha (TGF-α), from binding and activating the receptor (21). Cetuximab is an anti-EGFR mAb and is currently the only Food and Drug Administration (FDA)-approved molecularly targeted therapy for HNSCC (12, 13). Due to its success in clinical trials, cetuximab in combination with radiation has become a standard therapy for patients with HNSCC, as well as in combination with chemotherapy for patients who have

recurrent and/or metastatic HNSCC (12, 13). The second approach to inhibit EGFR is through the intracellular tyrosine kinase domain. Tyrosine kinase inhibitors (TKIs) are small molecules which act by blocking the adenosine triphosphate (ATP) binding site, thereby inhibiting phosphorylation of EGFR and further activation of downstream intracellular signaling pathways (6, 21). Erlotinib, an EGFR TKI, has had promising Phase II study results, and remains in active development for HNSCC (22). Targeted therapy in HNSCC in combination with chemotherapy and/or radiation has shown increased efficacy when compared to chemotherapy and radiation alone (12, 13). Improvements in overall survival have been achieved, although only minimal, and the mortality rate of HNSCC patients still remains high. It is evident that strategies that differ from the current methods of treatment are warranted.

1.3. Chemoprevention

The concept of cancer chemoprevention denotes the use of an agent; artificial, natural, or biological, to reverse, slow or arrest the process of carcinogenesis (23). Chemoprevention can be categorized into primary, secondary or tertiary prevention. Primary prevention involves preventing initial cancer in healthy individuals who are at risk, secondary prevention refers to preventing cancer in patients with lesions characteristic of premalignancy, and tertiary prevention is inhibiting a second primary cancer in patients cured of a previous cancer (24). The first FDA-approved primary prevention agent was tamoxifen, an estrogen receptor antagonist, which is used in the prevention of breast cancer. Clinical trial studies with tamoxifen in women with early-stage breast cancer showed overall survival benefit in patients that had taken tamoxifen for 5 years and decreased risk of recurrence (25, 26). Celecoxib, another FDA-approved chemoprevention agent, is currently used for the control of familial adenomatous

polyposis (27). More recently, there has been a focus on developing chemoprevention regimes in head and neck cancer, specifically oral cancer, where premalignant lesions can be more easily detected. It is well documented that head and neck carcinogenesis represents a step-wise progression to the development of invasive cancer (28-30), and methods of delaying or stopping the progression of the disease would provide great benefits to the head and neck patient population.

1.4. Chemoprevention of Head and Neck Cancer

Both secondary and tertiary prevention, targeting of premalignant lesions and intervention in patients at high risk for development of a second primary tumor, respectively, are very relevant for head and neck cancer patients. Various types of agents have been studied in chemoprevention of head and neck cancer including retinoids (vitamin A derivatives) and inhibitors of molecular targets such as anti-EGFR agents and cyclooxygenase 2 (COX-2) inhibitors (31-41). As previously stated, the EGFR is commonly overexpressed in head and neck cancer. In addition, activation of the EGFR is considered to be an early event in HNSCC carcinogenesis (16, 42, 43). Increased production of EFGR mRNA has been reported in pathological samples of normal mucosa from patients at risk for primary or secondary head and neck cancers with increased expression seen throughout progression to invasive cancer (16). These observations have led to preclinical and clinical investigations of EGFR as a target for chemoprevention (44, 45). Clinical investigation of the chemopreventive efficacy of erlotinib and cetuximab is currently ongoing in HNSCC patients with advanced premalignant lesions of the upper aero-digestive tract (46, 47). A recent chemoprevention study by Rosenthal *et al*. examined erlotinib as an adjuvant in head and neck cancer patients who had undergone salvage

surgery after recurrence. The trial highlighted poor tolerance to long-term erlotinib treatment at 150 mg (daily) (37). Given that chemoprevention strategies require long-term intervention, agents with low toxicity profiles offer an attractive approach in the prevention of HNSCC. Using dietary or natural supplements has the potential for long-term use and minimized toxicity compared to the standard chemotherapeutic agents. As previously mentioned, clinical studies have investigated vitamin A derivatives in chemoprevention of HNSCC, however, mixed outcomes and development of resistance to these agents has demonstrated difficulties in clinical application (34, 35). Due to the toxic effects of high dosing of single agents, development of resistance to single agents, and the aggressive nature of HNSCC, combination strategies that dual-target active signaling pathways or synergistically inhibit cancer progression are currently the most promising approach in chemoprevention (45, 47). Furthermore, the use of natural compounds or nutritional supplements as potential 'bio-adjuvants' for cancer prevention have become increasingly attractive (44, 48). In the present study, we examined the impact of calcitriol, the active metabolite of the nutritional supplement vitamin D_3, as a bio-adjuvant on the chemopreventive efficacy of erlotinib against oral cancer.

1.5. Role of Vitamin D in Cancer

Vitamin D is a steroid hormone that can be obtained from dietary sources or synthesized from 7-dehydrocholesterol in the skin following UV light exposure (49). The precursor form of vitamin D is transported through the circulation to the liver where it is hydroxylated to 25-hydroxycholecalciferol and then further hydrolyzed in the kidneys to 1,25-dihydroxycholecalciferol (1,25-$(OH)_2D_3$) or calcitriol (49, 50). Vitamin D has effects on bone and mineral metabolism and is also involved in the proliferation and differentiation of various

types of cells and tissues (49, 50). In addition to findings on the physiological role of vitamin D, various epidemiological studies indicate that vitamin D could serve as a potential risk-modifying factor in cancer (50, 51). *In vitro* studies in breast cancer, prostate cancer, and SCC cell lines have documented calcitriol's growth inhibitory effects (52, 53). Vitamin D has been widely studied as a chemopreventive agent in a variety of other cancers such as colorectal cancer, prostate cancer, and breast cancer (54-56). The diverse biological effects of vitamin D on cell proliferation, apoptosis, inflammation and angiogenesis, make it an attractive anti-cancer agent (52, 53, 56-58). Given the aggressive nature of head and neck tumors, combination strategies targeting multiple aspects of the tumor's biology, such as overexpression of the EGFR, angiogenesis, inflammation, and cell proliferation, should have significant therapeutic impact.

CHAPTER 2. PROJECT GOAL

The overall goal of this project was to examine the impact of calcitriol (1,25-dihydroxyvitamin D_3) on the chemopreventive efficacy of erlotinib against oral cancer.

2.1. Rationale and hypothesis

As previously mentioned, studies have found EGFR activation to be an early event in HNSCC carcinogenesis, leading to increased activation of downstream intracellular signaling pathways, such as the ERK-MAPK and PI3-AKT pathways, which are critically involved in cell growth, cell survival, and angiogenesis (59). Calcitriol has demonstrated to have interactions with these downstream signaling pathways through a decrease in the phosphorylation of Akt and Erk that is necessary for their activation, in addition to its activity inducing apoptosis (60). Based on this knowledge, we **hypothesized** that targeting EGFR and interacting signaling pathways using calcitriol in combination with the EGFR inhibitor, erlotinib, will result in improved suppression of oral cancer.

2.2. Specific Aims

Two specific aims were developed to test the hypothesis previously mentioned.

Specific Aim 1: To non-invasively characterize HNSCC progression in the 4NQO model using MRI.

Specific Aim 2: To examine the impact of calcitriol on the chemopreventive efficacy of erlotinib against oral carcinogenesis in the 4NQO model.

2.3. Approach

Conducting clinical trials of chemopreventive agents is a challenging endeavor. The financial burden, as well as maximal patient compliance, can be problematic. Therefore, the importance of preclinical investigation in models that simulate the multi-stage progression of carcinogenesis in humans cannot be emphasized enough. Published literature has documented that the molecular events and carcinogen-induced changes in mice after 4NQO exposure mimic the changes that occur in humans throughout and after carcinogen exposure (61). We conducted preclinical studies of our chemoprevention strategy using this model of oral carcinogenesis in mice. We used non-invasive MRI in conjunction with histologic and molecular analyses to assess the chemopreventive impact of our combination strategy.

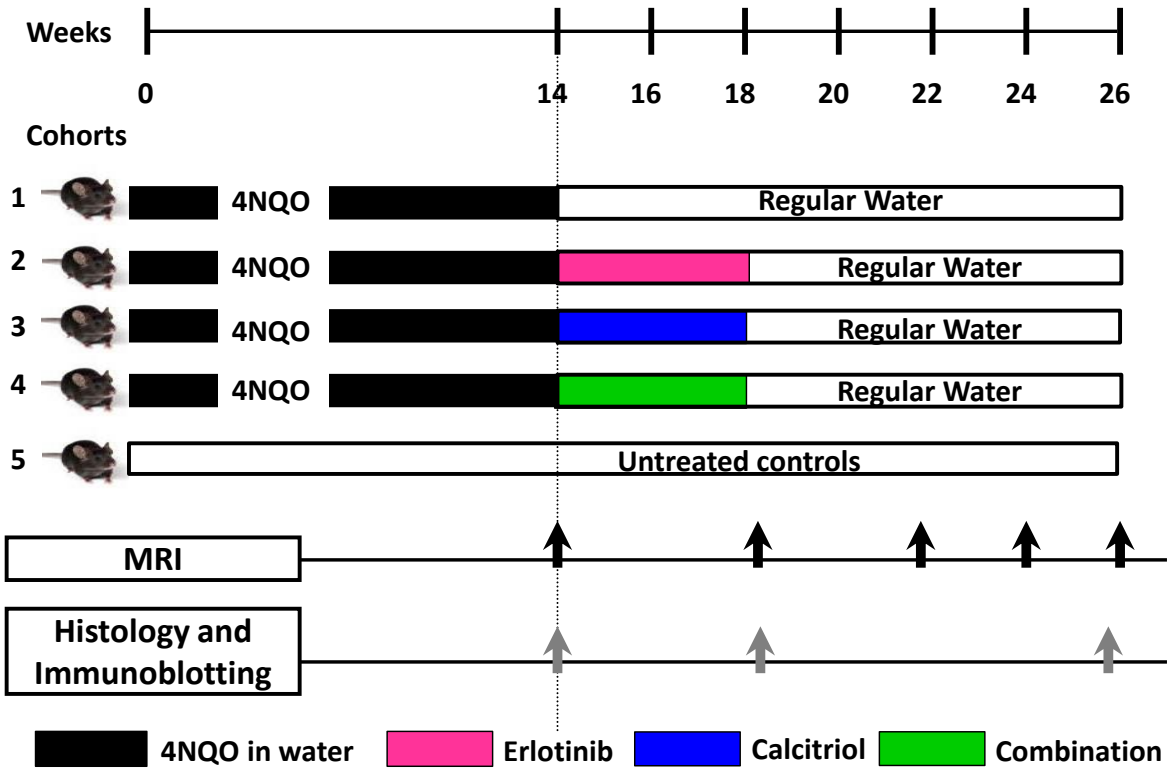

Figure 1. Experimental Design. The experimental design and the cohorts evaluated in the study. Following 14-week exposure to the carcinogen, 4NQO, animals were randomized into one of four arms: control, erlotinib alone, calcitriol alone or combination (n = 12-13 per group). Tumor presence was assessed through white-light visual examination of the oral cavity at various time points. Non-invasive magnetic resonance imaging (MRI) was performed at week 14 (following carcinogen exposure and prior to treatment); n = 7-9 per group, at week 18 (at the end of 4 weeks of treatment); n = 11-13 per group, and at week 26 (8 weeks post completion of treatment); n = 12-13 per group. Naïve animals (n = 3) were also imaged with MRI at weeks 0 and 26. Immunoblot analysis was carried out in a subset of animals (n = 3 per group) at weeks 18 and 26. Histopathologic assessment was carried out at week 18 (n = 4-5 per group) and week 26 (n = 7-9 per group). Imaging data is comprised of a collection of data from multiple studies.

CHAPTER 3. MATERIALS AND METHODS

3.1. Animal Model System. Four-to-six week old female C57Bl/6 mice were purchased from the National Cancer Institute (Rockville, MD). Animals were housed in cages in a laminar flow unit under ambient light and provided with food and water. The carcinogen, 4NQO (Sigma, St. Louis, MO), was dissolved in propylene glycol at 50 mg/ml and added to the drinking water at a final concentration of 100 μg/ml. Animals were administered 4NQO in their drinking water for 14 weeks. The water was changed *ad libitum* every 7-10 days. Regular autoclaved water was provided following completion of the 14-week period of carcinogen exposure. Control animals received autoclaved water at all times. This protocol for carcinogen exposure was based on published reports in the literature that have demonstrated consistent formation of lesions in this model that progress through various stages of carcinogenesis (62). All experimental procedures were performed in accordance with protocols approved by the Institutional Animal Care and Use Committee (IACUC) at Roswell Park Cancer Institute (RPCI).

3.2. Treatments. Erlotinib (Tarceva®) powder (Selleck Chemicals, Houston, TX) was dissolved in dimethyl sulfoxide (DMSO) at a concentration of 5 mg/ml and administered by oral gavage 25 mg/kg (5 days/week for 4 weeks). Calcitriol, 1,25-dihydroxyvitamin D_3, (Hoffman-La Roche, Inc., Nutley, NJ) was kindly provided by the laboratory of Candace S. Johnson of the Pharmacology and Therapeutics Department at RPCI. Calcitriol was reconstituted in 100% ethyl alcohol then diluted in phosphate-buffered saline to a final concentration of 1 μg/ml and administered 0.1 μg per mouse (3 days/week for 4 weeks) by intraperitoneal injection.

3.3. Imaging-Based Assessment

3.3.1. Magnetic Resonance Imaging. Experimental MRI examinations were performed using a 4.7 T/33-cm horizontal bore magnet (GE NMR Instruments, Fremont, CA) incorporating AVANCE digital electronics (Bruker Biospec with ParaVision 3.0.2; Bruker Medical Inc., Billerica, MA) and a removable gradient coil insert (G060, Bruker Medical Inc., Billerica, MA) generating maximum field strength of 950 mT/m and a custom-designed 35-mm RF transmit-receive coil. Animals were anesthetized using 2.5% Isoflurane (Benson Medical Industries, Markham, ON, Canada) prior to and during imaging. The mice were secured in a form-fitted, MR compatible sled (Dazai Research Instruments, Toronto, Canada) equipped with temperature and respiratory monitoring sensors. The sled, along with a phantom containing 0.15 mM gadopentetate dimeglumine (Gd-DTPA; Magnevist, Berlex Laboratories, Wayne, NJ), was positioned inside the scanner using a plastic carrier tube. Animal body temperature was maintained at 37°C during imaging using an air heater system (SA Instruments Inc., Stony Brook, NY), and automatic temperature feedback was initiated through thermocouples in the sled, in conjunction with computer software supplied with the heater. Transverse axial multi-slice, two-dimensional T2-weighted (T2W) spin echo images incorporating RARE (rapid acquisition with relaxation enhancement) encoding were acquired for each mouse using the following parameters: matrix size 256 x 192, TE/TR = 41/2500 ms, slice thickness 1 mm, field of view (FOV): 3.2 x 3.2 cm, number of slices = 20, acquisition time = 4 minutes. T2W images were acquired at different time points throughout and post 4NQO exposure. Post processing of raw datasets was performed using the medical imaging software, Analyze PC (Version 8.0, AnalyzeDirect, Overland Park, KS. A region of interest (ROI) was traced around the entire tumor on each slice on T2-weighted images and saved as an object map. Tumor volume was

calculated measuring the cross sectional area on each slice and multiplying this area with slice thickness and the number of slices.

3.3.2. White Light Digital Imaging. For confirmation of MRI results and assessment of visual changes in tongue morphology, white light images were acquired every two weeks throughout the course of the study. For *in vivo* imaging, mice were anesthetized using 2.5% isoflurane prior to imaging and visual inspection. For *ex vivo* analysis, animals were humanely sacrificed and tongues were resected immediately prior to imaging.

3.4. Immunohistochemistry and Histology. Whole tongue specimens were fixed in 10% neutral-buffered formalin (Sigma, CA) for immunostaining and histology. Immunostaining of whole tongue sections for the vitamin D receptor (VDR) was performed using the monoclonal antibody 9A7 (MA1-710; Thermo Fisher Scientific Pierce Antibody Products, Rockford, IL) by the Mouse Tumor Model Resource at RPCI. Relative VDR expression was qualitatively analyzed based on intensity of the stain within a given 20x magnification field. The Pathology Resource Network at RPCI performed the tissue sectioning on all tissue samples for H&E staining. All samples were paraffin-embedded and cut at 4 μm, placed on charged slides, and dried. For H&E staining performed in the Seshadri lab, slides were deparaffinized in two changes of xylene, followed by multiple rehydration steps of different ethyl alcohol concentrations and lastly with distilled water. Nuclei were stained with Harris Hematoxylin (Sigma, St. Louis, MO), rinsed in running tap water and then differentiated with 1% acid alcohol. Slides were rinsed in running tap water for four minutes for bluing, followed by a rinse in 95% ethyl alcohol. Next, the slides were stained with Eosin (Sigma, St. Louis, MO) for one minute. A

series of dehydration steps in three changes of alcohol occurred followed by three changes of xylene to clear the slides. Lastly, the slides were cover slipped. All slides were scanned and digitized using the Scanscope XT system (Aperio, Vista, CA) and images were captured using the ImageScope software. H&E stained sections of the tongue were examined by a board-certified pathologist with a clinical practice focus in head and neck cancer, blinded to therapeutic arm, imaging findings and outcome. Histologic assessment of hyperkeratosis (thickened keratinized layer), dysplasia grade (architectural disarray, increased nuclear to cytoplasmic ratio, hyperchromatic nuclei, increased or abnormal mitotic figures), and invasive carcinoma (frank invasion into the connective tissue stroma) was conducted as described previously (63).

3.5. Immunoblotting. Animals were humanely sacrificed and whole tongues excised and flash frozen for molecular analysis at various time points post carcinogen exposure. Expression levels of VDR and phosphorylated forms of EGFR and Akt in tissues were measured by immunoblotting of whole tongue extracts using primary antibodies specific for these markers. Protein extracts of whole tongue tissue were prepared by manually homogenizing the tissue with a mortar and pestle to a fine powder and adding TX-100/SDS lysis buffer, phosphatase inhibitor cocktail (CalBioChem, Billerica, MA) and protease inhibitor. Protein extracts were kept on ice for 30 minutes and vortexed at 10 minute intervals. Lysates were clarified by centrifugation for 10 minutes at 4 ºC and protein concentrations were determined using the BCA protein assay (Thermo Scientific, Waltham, MA). Proteins were resolved using SDS-PAGE and transferred to PVDF membranes. Western blots were performed using the following primary antibodies: monoclonal rat anti-VDR (clone: 9A7; Thermo Fisher Scientific, Waltham, MA), monoclonal rabbit anti-phospho-EGFR (phospho Y1092; abcam, Cambridge, MA), polyclonal rabbit anti-

phospho-AKT1 (phospho S473; abcam, Cambridge, MA). Anti-rabbit and anti-mouse horseradish-peroxidase-conjugated secondary antibodies (GE Healthcare, Pittsburgh, PA) were used and blots were developed using enhanced chemiluminescence. Actin (I-19; Santa Cruz, Dallas, TX) was used in each experiment as a loading control. To assess differences in protein expression, western blot films were analyzed using the UN-SCAN-IT program (Silk Scientific, Inc., Orem, UT). Equal sized regions of interest (ROIs) were fitted around each expression band to measure total pixels. Using the total pixels acquired from the blot and the total pixels acquired from the corresponding actin blot, a normalized expression value was achieved [(antibody total pixels/actin total pixels)/average control tissue expression].

3.6. Toxicity Assessment. Animals were monitored according to changes in wellness including: decreased mobility, weight loss, and difficulty eating/drinking, upon which displaying the listed symptoms, were euthanized. Body weight measurements were obtained three times weekly during and after intervention. Animals were humanely euthanized when sustained loss of body weight (≥20% of initial body weight) was observed. In addition, cardiotoxicity was assessed by ultrasound imaging. Cardiac imaging was performed with the Vevo® LAZR (VisualSonics Inc., Toronto, ON, Canada) system with a 55MHz ultrasound transducer. Mice were anaesthetized with 2% isoflurane and secured to the heated imaging platform. The animal's forelimbs and hindlimbs were taped to the ECG leads to acquire the heart rate of the animal. The platform was tilted forward and angled to allow optimum visualization of the left ventricle. Once in position, gel was placed on the chest of the animal and the transducer was lowered into position. To obtain a parasternal long axis view, the transducer was tilted forward and rotated 35° counter-clockwise. Cardiac imaging mode was activated and long axis images were acquired for 100

frames. From this position, the transducer was rotated 90° clockwise to obtain a parasternal short axis view of the heart. The left ventricle was broken up into four quadrants down the length of the ventricle and each quadrant was imaged during systole and diastole. Following acquisition of datasets, the Vevo® 2100 processing suite was used to perform a Simpson measurement of the heart. First, the three lower quadrants on the short axis were analyzed by tracing out the endocardium at diastole and systole. For the long axis view a line was drawn from the endocardium at the apex of the heart to the entrance of the aorta during systole and diastole. Parameters of cardiac function [ejection fraction (EF), cardiac output (CO), and stroke volume (SV)] were calculated by the VevoCQ image processing software (VisualSonics Inc., Toronto, ON, Canada).

3.7. Statistical Considerations. All statistical analyses were measured using GraphPad version 6.00 for Windows (Graphpad Software, San Diego California USA, www.graphpad.com). Measured values were reported as the mean ± standard error of the mean. Tumor volume calculated from MRI and percentage of animals with tumor visible on MRI were reported. For imaging studies and western blot analyses, mean tumor volume comparisons between different cohorts and difference in protein expression between the cohorts were analyzed using one-way ANOVA statistical tests. Tabulated data reporting incidence of tumor on MRI, incidence of dysplasia and incidence of invasive SCC through histopathologic assessment was analyzed using the Fisher exact probability test. P-values of <0.05 were considered statistically significant.

CHAPTER 4. RESULTS

4.1. Characterization of HNSCC progression in the 4NQO model

4.1.1. Non-invasive MRI of oral carcinogenesis *in vivo*

We performed serial magnetic resonance imaging (MRI) to non-invasively monitor oral carcinogenesis in the 4NQO model. T2-weighted MRI was performed at 14 weeks (immediately after completion of carcinogen exposure) and follow up scans were acquired at weeks 18, 22, 24 and 26. **Figure 2** shows T2-weighted axial images of naïve (**Figure 2A**) and 4NQO-treated animals (**Figure 2B**) at different time points after carcinogen exposure. Exposure to 4NQO resulted in morphologic changes in the oral cavity that included thickening of the borders of the tongue (*outlined*, **Figure 2B**) as well as development of exophytic lesions on the dorsal surface (*arrow*, **Figure 2B**). **Figure 2D** demonstrates the morphologic changes throughout the whole tongue that occurred by week 26 in 4NQO-treated animals compared to naïve controls (**Figure 2C**). When comparing the enlarged images of the tongues in the anterior slices, thickening of the tongue's ventral and lateral borders can be observed (*outlined in red*, **Figure 2C**, **D**). The middle-posterior slices show thickening on the dorsal surface of the 4NQO-treated tongue (hyperintensive regions), possibly indicative of hyperplasia or dysplasia, as well as presence of an exophytic growth (*arrowhead*, **Figure 2D**). MRI offers a safe, non-invasive method to detect morphological changes in the oral cavity during the carcinogenesis process following 4NQO exposure, confirming the application of this model to our studies.

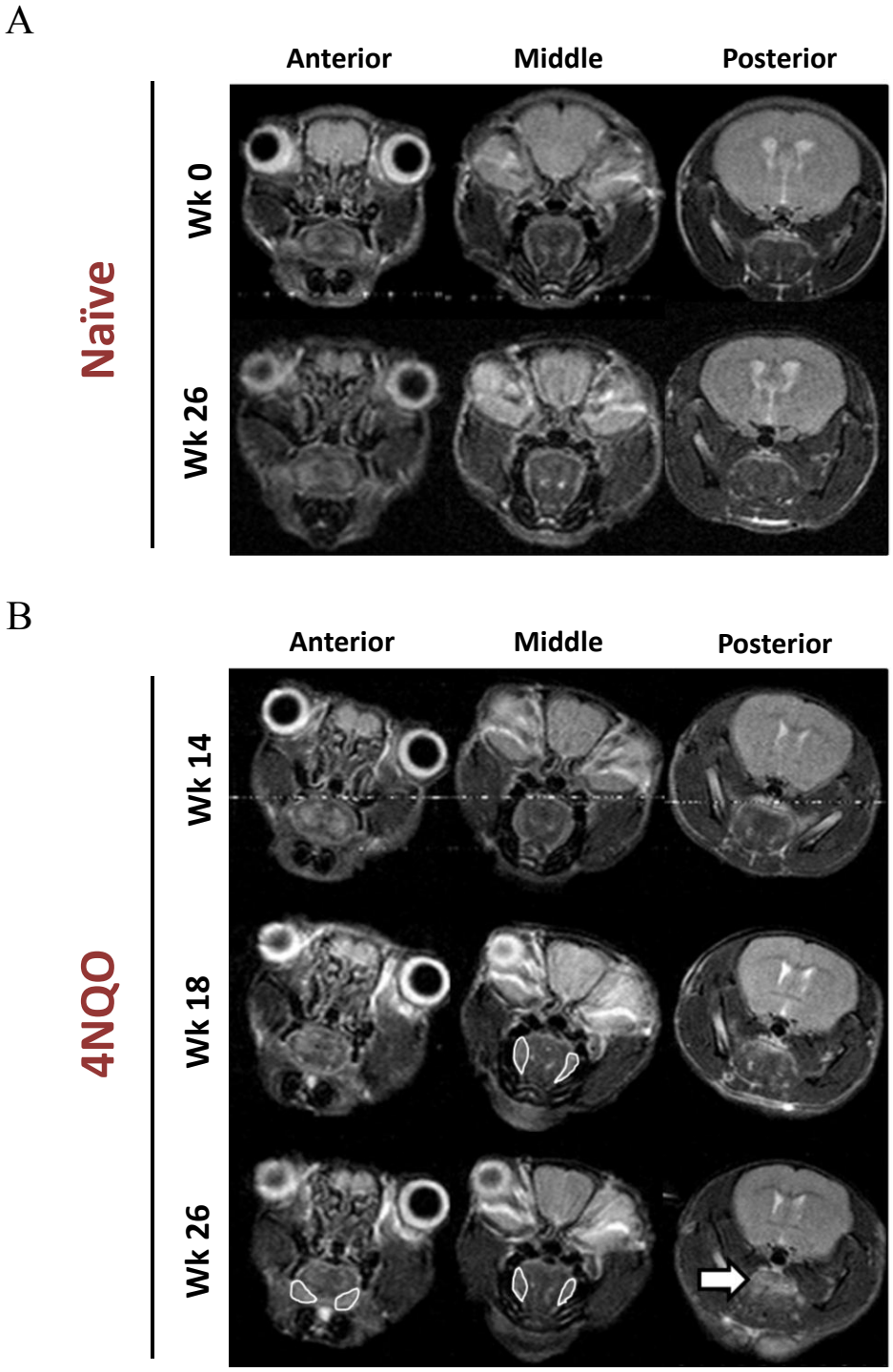

Figure 2. MRI of 4NQO-induced oral carcinogenesis. (A) T2-weighted axial images of a naïve C57Bl/6 mouse at the beginning of the study, week 0, and at the end, week 26. **(B)** T2-weighted axial images of a C57Bl/6 mouse at various time points following exposure to the carcinogen, 4NQO.

C

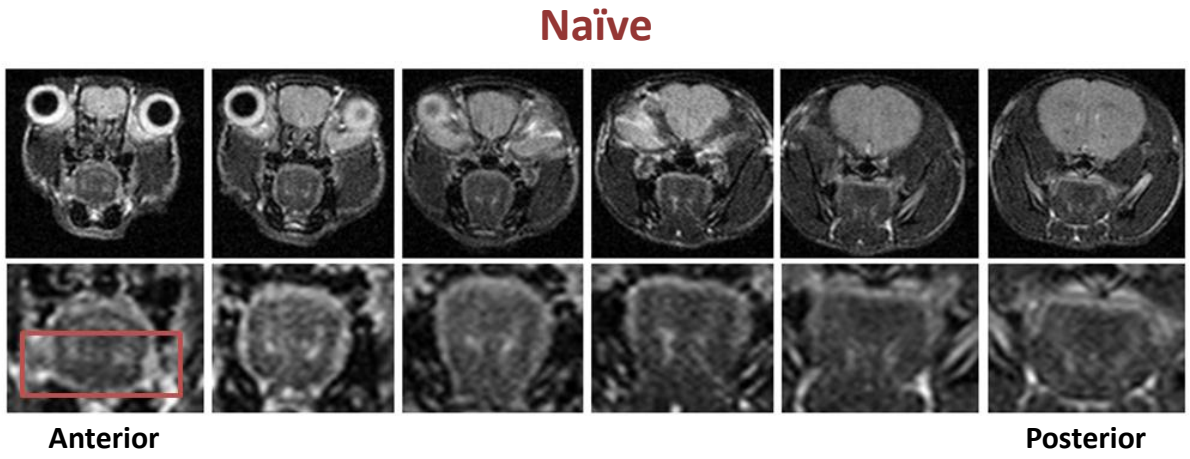

D

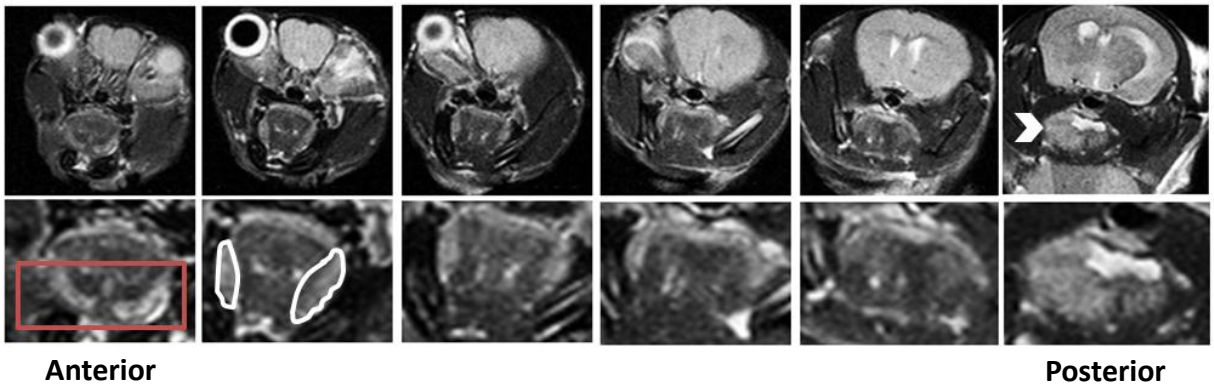

Figure 2. MRI of 4NQO-induced oral carcinogenesis. (C) T2-weighted axial images of a naïve mouse at week 26 and a 4NQO-treated mouse **(D)** at week 26. Images shown left-to-right represent MRI slices of the anterior portion of the mouse and tongue traveling further posteriorly through the mouse/tongue. Lower panel of images in **(C)** and **(D)** represent enlarged versions of the tongue shown directly above. Red outline in **(C)** and **(D)** highlight difference in thickening of the ventral border of the tongues. White outline in **(D)** shows lateral border thickening; white arrowhead shows dorsal surface solid tumor.

4.1.2. Digital imaging of oral carcinogenesis *in vivo*

Serial white-light digital images were acquired in addition to MRI for confirmation of findings. **Figure 3A** illustrates the progression of carcinogenesis *in vivo* throughout the study. Leukoplakia and dysplastic-looking lesions developed post-completion of carcinogen exposure. Increased thickening of the tongue, in addition to development of white lesions were visible by week 23 and week 26 (*arrows*, **Figure 3A**) and exophytic growths on the tongue were present by week 26 (*outlined*, **Figure 3A**). No changes based on visual examination were seen in the naïve tongues over time. **Figure 3B** shows the corresponding *in vivo* and *ex vivo* digital images at the end point of the study (week 26), as well as corresponding whole tongue H&E sections of the naïve and 4NQO-treated tongue in addition to the matching T2 axial MRI. Presence of solid tumor is identified on MRI (*arrow*, **Figure 3B**) and by digital imaging (*outline*, **Figure 3B**). Consistent with the imaging data, histologic assessment of the 4NQO-treated tongue confirmed dysplasia and focal invasive squamous cell carcinoma (**Figure 3B**) at week 26.

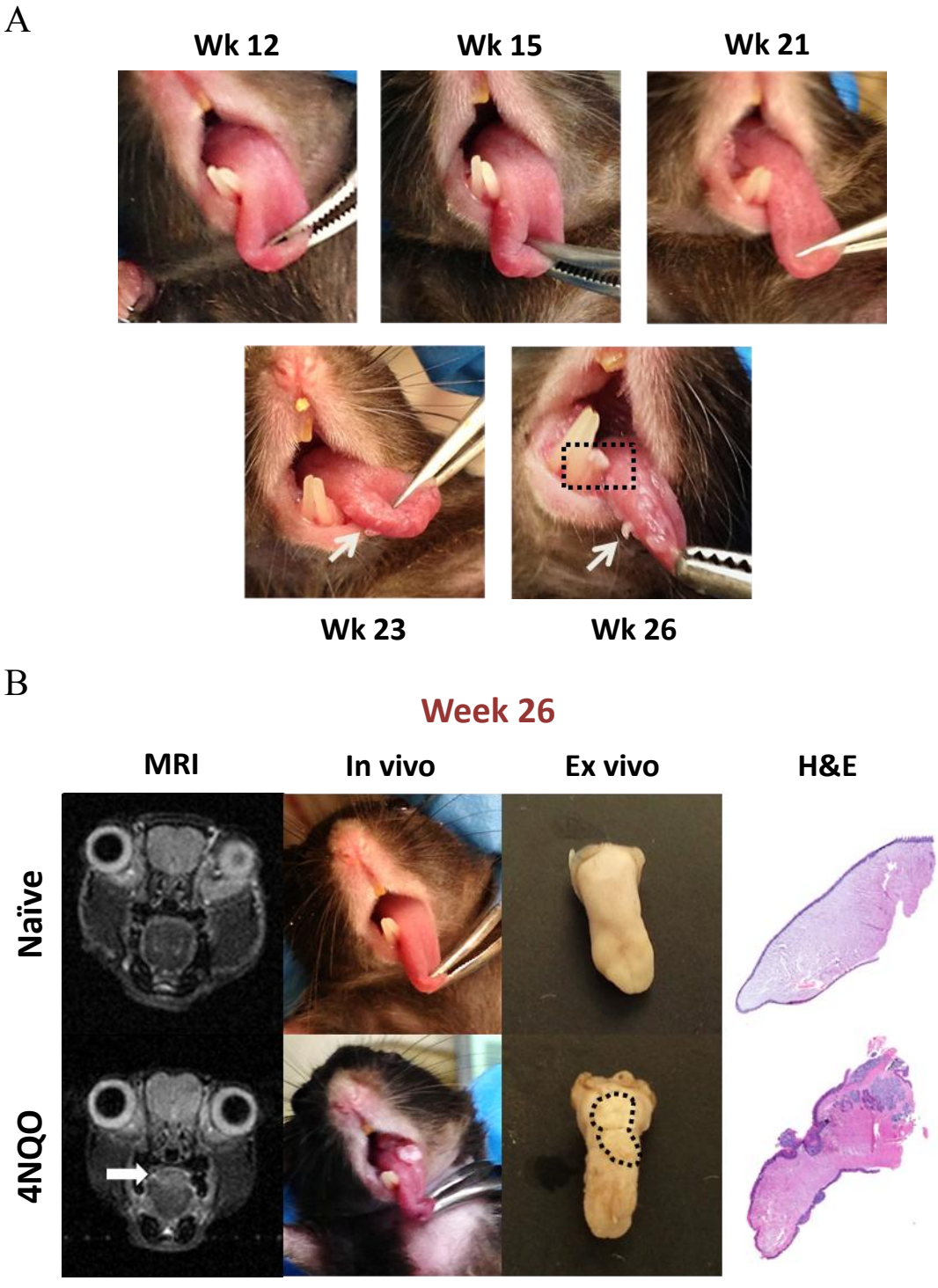

Figure 3. 4NQO-induced oral carcinogenesis. (A) Serial digital images of a 4NQO-treated tongue during carcinogen exposure (week 12) and after (weeks 15, 21, 23 and 26). Outlined black box highlights development of tumor growth on the right lateral border/floor of the mouth at week 26. **(B)** T2-weighted axial MRI images of a naïve mouse and a 4NQO-treated mouse at week 26. *In vivo* and *ex vivo* photomicrographs and histologic sections of the corresponding tongues are shown for comparison of the carcinogen-induced changes.

4.1.3. Immunohistochemical evaluation of vitamin D receptor expression in the 4NQO model

To determine whether the 4NQO model of oral cancer expressed the receptors our chemopreventive agents were targeting, we performed immunohistochemical analyses on naïve (untreated) tongues of C57Bl/6 mice as well as tongues treated with 4NQO to determine the vitamin D receptor status. The effects of calcitriol are primarily mediated through its interactions with the vitamin D receptor (VDR). The VDR is expressed in several tissues as well as in multiple types of cancer cells (57, 64, 65). In addition, upregulation of VDR has been previously observed with disease progression (66). We therefore performed immunohistochemical analyses on naïve and 4NQO-exposed tongues to determine the VDR status in our experimental system. No confirmation of expression of the epidermal growth factor was necessary due to findings in previous published work stating that 4NQO causes increased expression of the EGFR in a rodent model, consistent with the pathology of head and neck cancer in humans (61). The panel of images shown in **Figure 4** represents photomicrographs of VDR-stained sections of tongues obtained from naïve and 4NQO-treated mice (*top panel*). Corresponding hematoxylin and eosin stained sections are also shown (*bottom panel*). Increased expression of VDR was seen in the 4NQO-exposed tongue (**Figure 4B**), particularly in regions exhibiting hyperplastic and dysplastic changes (**Figure 4E**), compared to the normal epithelium of naïve tongues (**Figure 4A**, **D**). Higher expression of VDR was also observed in regions of the 4NQO-treated tongue with invasive squamous cell carcinoma (**Figure 4C**, **F**) compared to the naïve untreated tongue (**Figure 4A**, **D**).

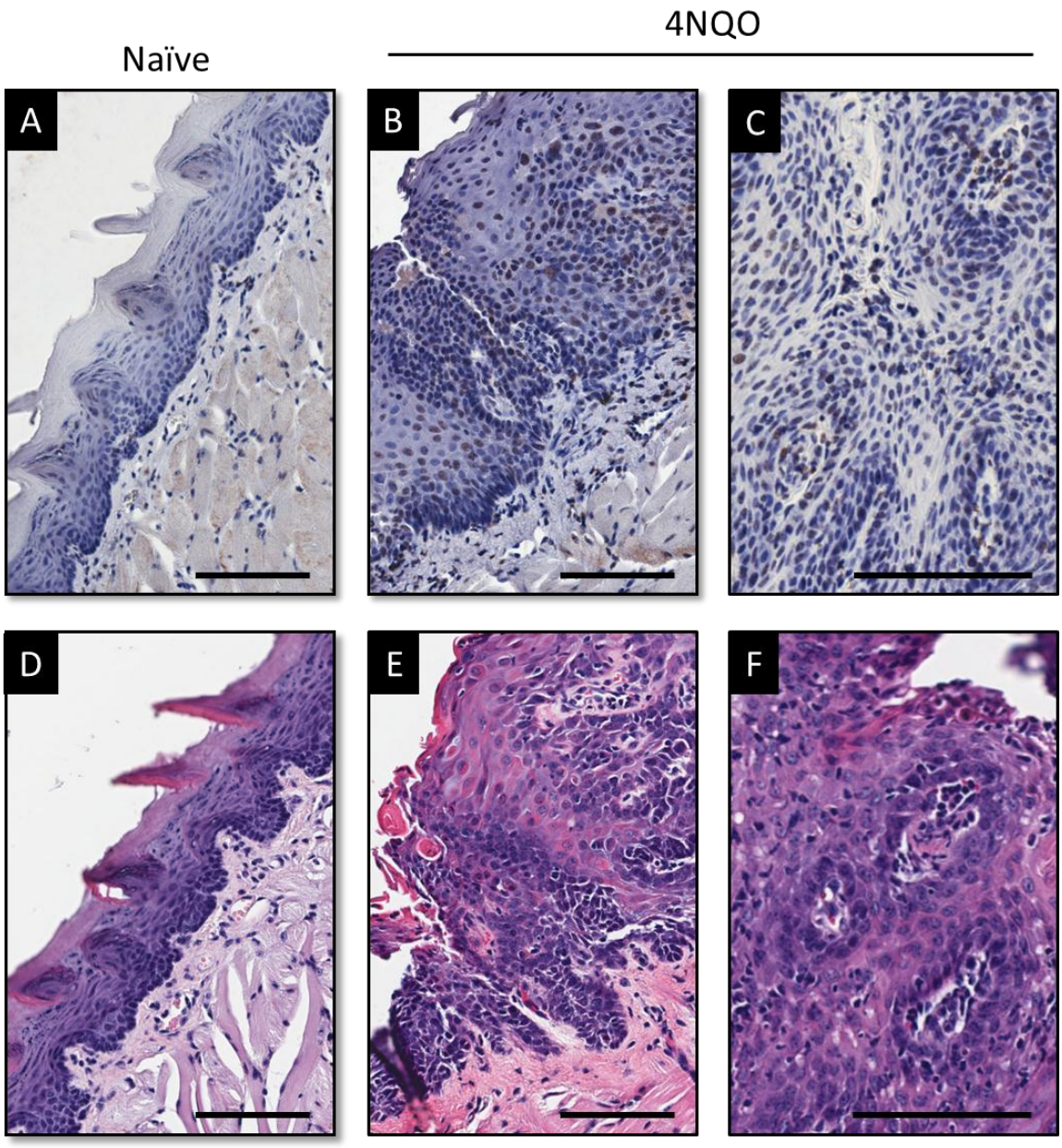

Figure 4. Vitamin D receptor expression in the 4NQO model. (A) VDR-stained untreated (naïve) tongue showing modest VDR expression and **(B)** VDR-stained tongue at week 26, 12 weeks post completion of 14 weeks of 4NQO exposure, showing increased VDR expression. **(C)** VDR-stained neoplastic lesion of the 4NQO-treated tongue, week 26. Corresponding H&E stained sections of the naïve tongue **(D)**, 4NQO-treated tongue **(E)**, and neoplastic lesion in 4NQO-treated tongue **(F)**. Magnification bars, 100 μm.

4.2. Chemoprevention of oral carcinogenesis with erlotinib and calcitriol

4.2.1. Longitudinal MRI of the effects of erlotinib and calcitriol on oral carcinogenesis

MR images were acquired at various time points throughout 4NQO exposure and post treatment of single agent erlotinib, single agent calcitriol, and combination to assess differences in cancer progression among the groups. Minimal changes were seen in tongue morphology prior to completion of 4NQO exposure (week 14) on MRI. Definitive changes in tongue appearance were identified on MRI beginning week 18 (immediately post completion of treatment with erlotinib, calcitriol, or combination). The panel of images shown in **Figure 5A** represents T2-weighted axial MR images of animals from each cohort at four time points. **Figure 5A** exhibits the changes induced by 4NQO exposure detectable by MRI, such as, thickening of the tongue on the dorsum and lateral borders, as well as development of solid tumor (indicated by the white arrows). Percentage of tumor incidence and quantification of tumor volume from MRI revealed differential changes in disease progression and tumor growth among all groups (**Figure 5B-F**). At week 18 (immediately following completion of 4 weeks of treatment), 5/11 animals in the control group showed presence of tumor on MRI while 6/11 animals in the calcitriol arm showed evidence of tumor upon imaging examination (one animal in the control arm and one animal in the calcitriol arm did not receive imaging at week 18). 1/13 animals in the combination treatment group had tumor visualized on MRI, and 1/12 animals treated with erlotinib alone showed presence of tumor on MRI examination at week 18. Tumor incidence (% of animals with tumor on MRI) increased in all four groups over time. By week 26, all control mice had detectable tumor, while mice treated with combination of erlotinib and calcitriol displayed a significantly lower incidence of tumor compared to controls (**Figure 5F**). Quantification of tumor volume by MRI was calculated at weeks 18, 22, 24, and 26 (n = 5-6 per group). Throughout the study, the

combination-treated mice exhibited a significantly lower mean tumor volume compared to tumor-bearing control mice (**Figure 5B-E**). In addition, single agent calcitriol had a higher mean tumor volume compared to control mice (**Figure 5B-E**).

A

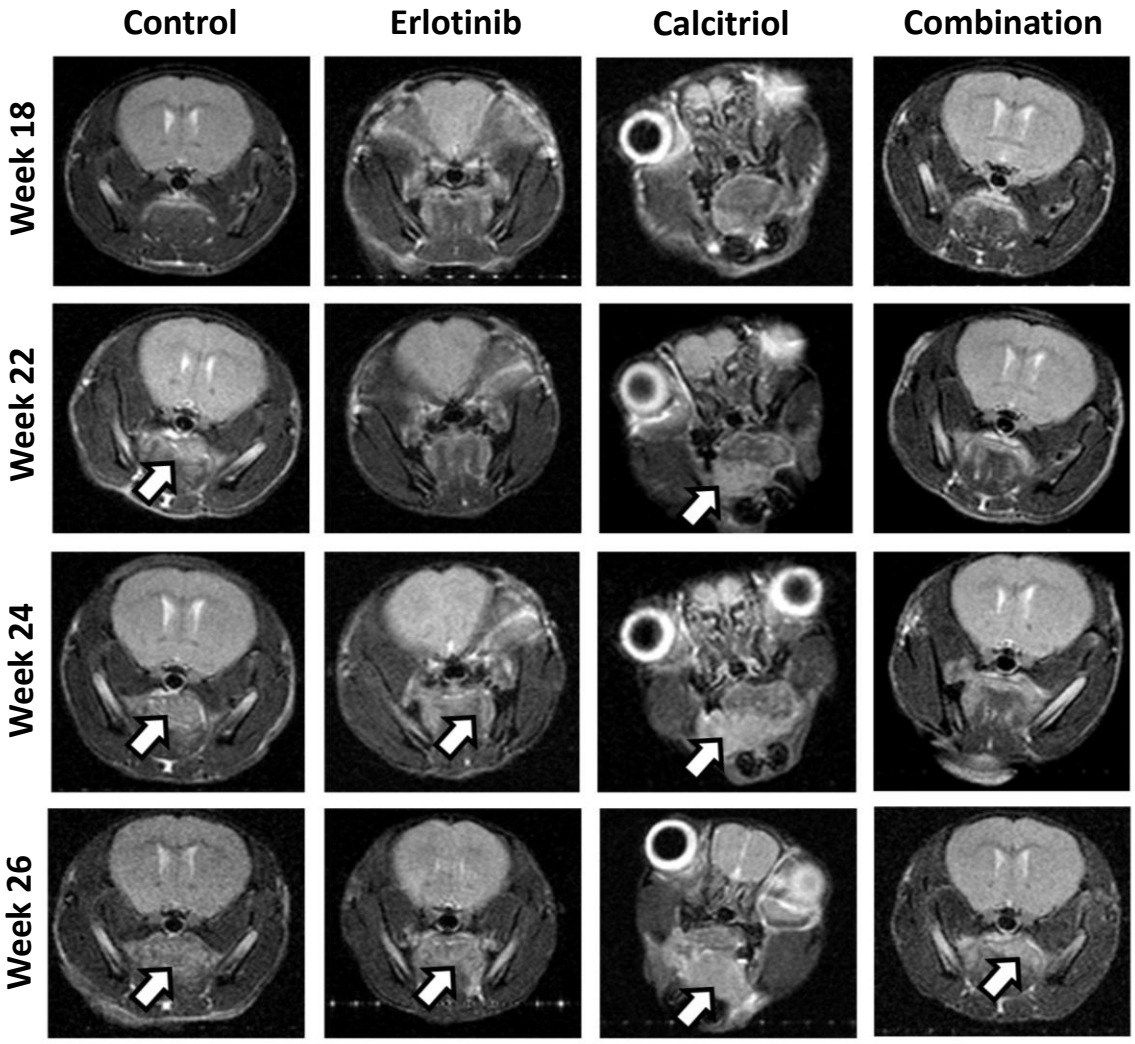

Figure 5. Assessment of treatment impact on oral carcinogenesis through MRI. (A) Serial T2-weighted axial MRI images of one mouse per treatment group at four time points; immediately after preventive intervention (week 18), to the end of the study (week 26). Animals received treatment for 4 weeks, following 14 weeks of 4NQO exposure. erlotinib was administered 25 mg/kg p.o, 5 days per week, calcitriol was administered 0.1 μg i.p, 3 times per week. Control animals were exposed to 4NQO for 14 weeks and received no further treatment.

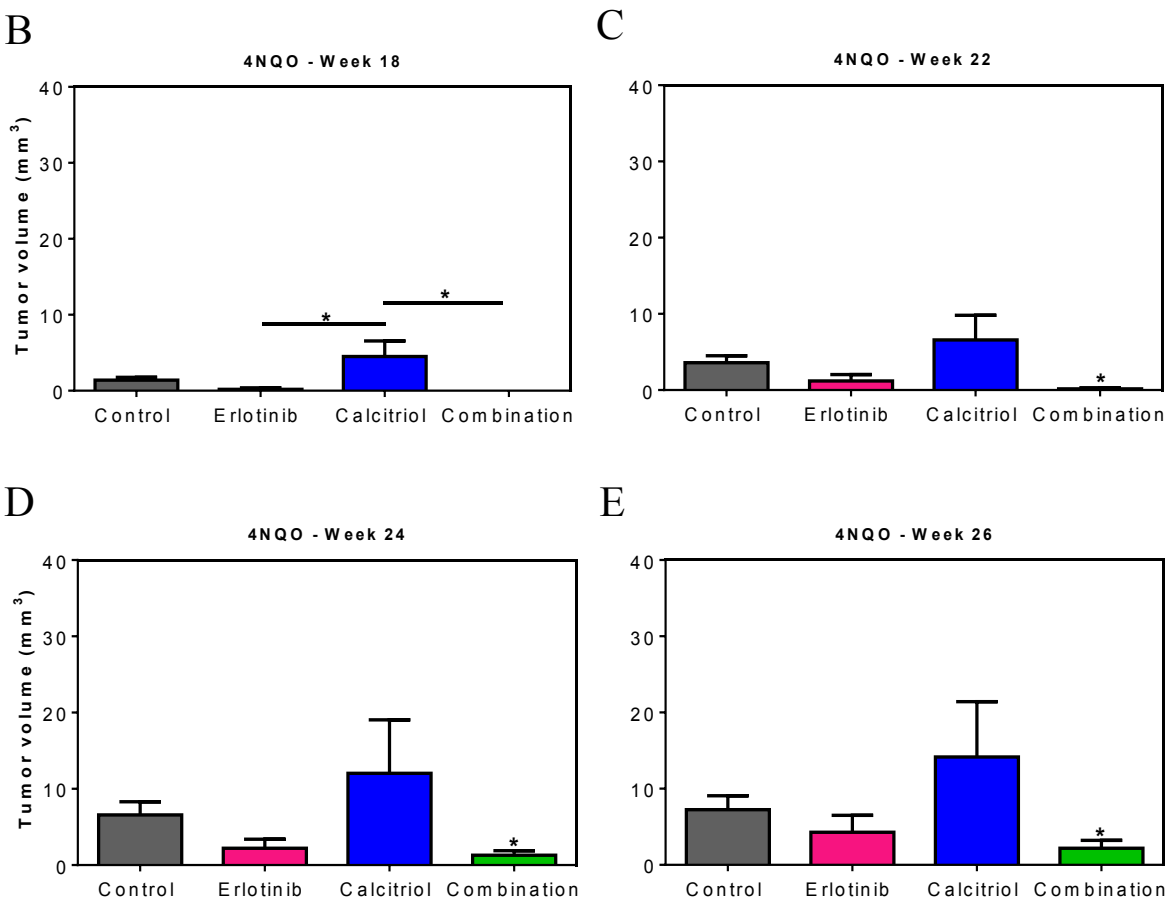

F

Group	Treatment	Incidence of visible lesions (%)-Wk18	Incidence of visible lesions (%)-Wk26
1	Drinking water only	0/3 (0)	0/3 (0)
2	4NQO only	5/11 (45.5)	12/12 (100)
3	4NQO + Erlotinib	1/12 (8.3)	8/12 (66.7)
4	4NQO + Calcitriol	6/11 (54.5)	11/12 (91.7)
5	4NQO + Erlotinib + Calcitriol	1/13 (7.7)	8/13 (61.5)*

*$P < 0.05$ compared to Group 2 (Fisher exact probability test)

Figure 5. Assessment of treatment impact on oral carcinogenesis through MRI. (B) – (E) Tumor volume measurements based on MRI; n = 5-7 per group; significance reported compared to control group ($p<0.05$). **(F)** Incidence of tumor detected by MRI weeks 18 and 26; n = 11-13 per group ($p<0.05$).

4.2.2. *Ex vivo* evaluation of the effects of erlotinib and calcitriol on oral cancer

Visual inspection of all tongues, in addition to white light digital imaging, occurred weekly throughout the duration of the study to monitor the carcinogenesis process among all groups. At the end point of the study (week 26), tongues were resected and analyzed for presence of tumor growth. Upon inspection of *ex vivo* tongues, quantity of visible lesions per tongue was recorded for each cohort (n = 7-9 per group). **Figure 6B** presents tongue lesion multiplicity by treatment group. Erlotinib single agent treatment and combination treatment with calcitriol exhibited significantly lower mean number of lesions per mouse compared to control mice (**Figure 6B**). "Lesions" were identified as growths protruding from the normal tongue musculature. **Figure 6A** displays representative images of *ex vivo* tongues from each cohort; lesions identified are outlined in black.

A

B

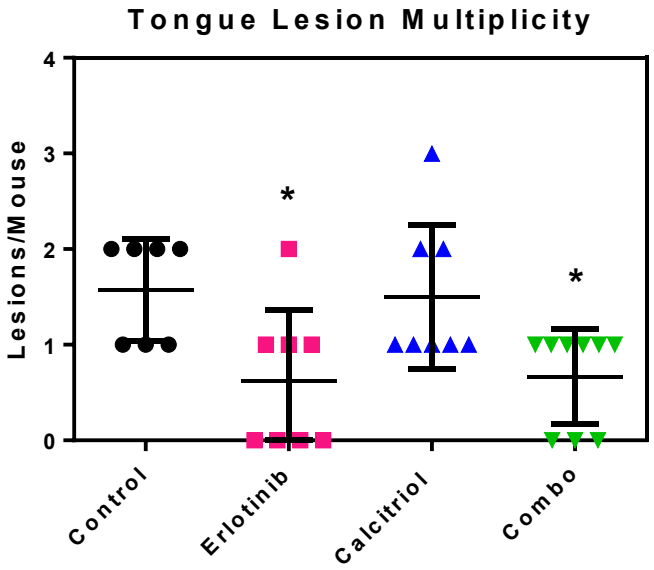

Figure 6. *Ex vivo* digital imaging analysis of tumor growth.
(A) *Ex vivo* digital images of one tongue per group at week 26. Lesions detected on tongues are outlined. **(B)** Quantification of lesion multiplicity per tongue by treatment group compared to control group ($p<0.05$).

4.2.3. Histopathologic evaluation of the impact of erlotinib and calcitriol on oral carcinogenesis

Histopathologic assessment of tissues was performed at weeks 18 and 26 to determine the effects of the preventive intervention on incidence and progression of pre-neoplastic and neoplastic lesions. Representative H&E-stained whole tongue sections obtained from an animal in each cohort at week 18 are shown in **Figure 7A**. At week 18, control mice exhibited the highest incidence of moderate-severe dysplasia, while combination-treated mice exhibited the lowest incidence of moderate-severe dysplasia (**Figure 7B)**. **Figure 8A** shows representative H&E stained whole tongue sections from an animal in each cohort at week 26. The control tongue shows presence of a papilloma in addition to severe dysplasia and focal invasive SCC (**Figure 8A**). Both control and calcitriol-treated tongues reveal additional thickening of the epithelium compared to tongues treated with either single agent erlotinib or combination (**Figure 8A**). Varying degrees of dysplasia were observed in the tongue post 4NQO exposure; however, the greatest effect on slowing progression of disease post treatment was seen in the combination-treated tongues. At week 26 (8 weeks post cessation of treatment), combination demonstrated decreased severity of dysplasia, having significantly higher incidence of mild dysplasia, as well as significantly lower incidence of moderate-severe dysplasia compared to controls (**Figure 8B**). Control tongues exhibited the highest incidence of invasive SCC (71.4%) on histopathologic examination. Calcitriol-treated tongues showed 62.5% incidence, while tongues treated with erlotinib both single agent and combination treatment exhibited a marked reduction in invasive SCC, 37.5% and 33.3%, respectively (**Figure 8B**).

A

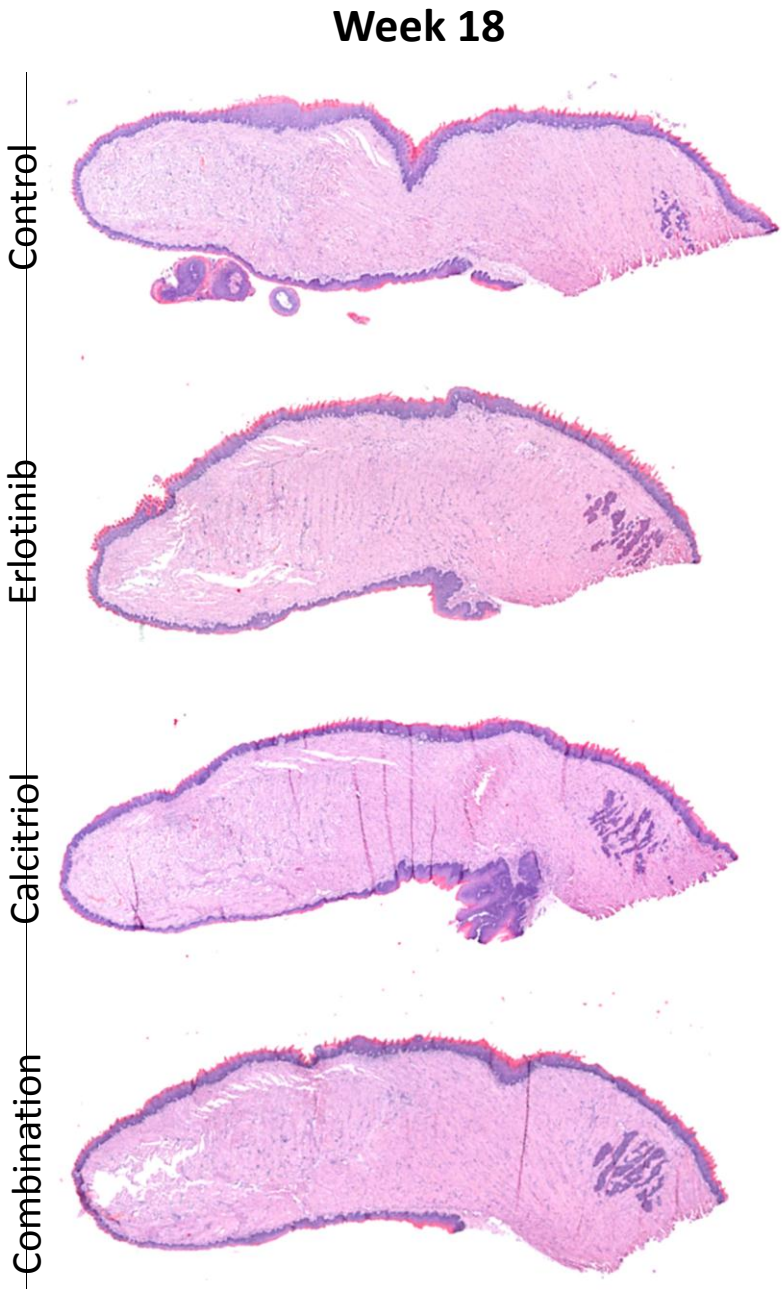

Figure 7. Histopathologic assessment of the chemopreventive efficacy of erlotinib-calcitriol combination treatment against oral carcinogenesis at week 18. (A) Images of hematoxylin and eosin stained mouse tongues (at week 18) 24 hours post completion of 4 weeks of treatment with erlotinib alone (25 mg/kg p.o, 5 days/week), calcitriol alone (0.1 µg i.p 3 times/week), combination treatment, or no treatment (control).

B

Group	Treatment	Mild dysplasia (%)	Moderate-Severe Dysplasia (%)	SCC (%)
1	4NQO only	0/4	4/4 (100)	1/4 (25)
2	4NQO + Erlotinib	1/5 (20)	4/5 (80)	2/5 (40)
3	4NQO + Calcitriol	1/5 (20)	4/5 (80)	4/5 (80)
4	4NQO + Erlotinib + Calcitriol	2/5 (40)	3/5 (60)	2/5 (40)

Figure 7. Histopathologic assessment of the chemopreventive efficacy of erlotinib-calcitriol combination treatment against oral carcinogenesis at week 18. (B) Incidence of dysplasia and incidence of invasive squamous cell carcinoma by treatment group.

A

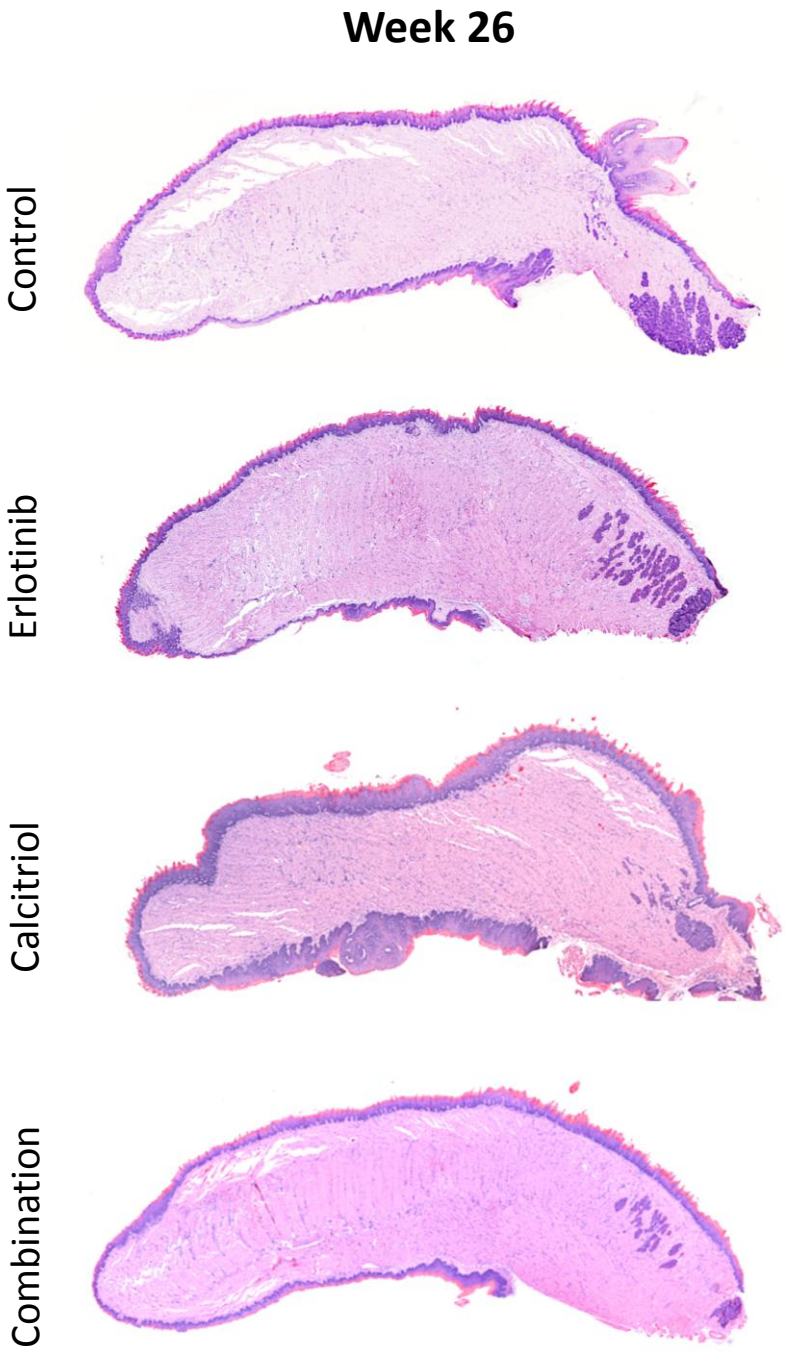

Figure 8. Histopathologic assessment of the chemopreventive efficacy of erlotinib-calcitriol combination treatment against oral carcinogenesis at week 26. (A) Images of hematoxylin and eosin stained mouse tongues (at week 26) 12 weeks post completion of 4 weeks of treatment with erlotinib alone (25 mg/kg p.o, 5 days/week), calcitriol alone (0.1 µg i.p 3 times/week), combination treatment, or no treatment (control).

B

Group	Treatment	Mild dysplasia (%)	Moderate-Severe Dysplasia (%)	SCC (%)
1	Drinking water only	0/3	0/3	0/3
2	4NQO only	0/7	7/7 (100)	5/7 (71.4)
3	4NQO + Erlotinib	2/8 (25)	6/8 (75)	3/8 (37.5)
4	4NQO + Calcitriol	1/8 (12.5)	7/8 (87.5)	5/8 (62.5)
5	4NQO + Erlotinib + Calcitriol	5/9 (55.6)*	4/9 (44.4)*	3/9 (33.3)

*$P < 0.05$ compared to Group 2 (Fisher exact probability test)

Figure 8. Histopathologic assessment of the chemopreventive efficacy of erlotinib-calcitriol combination treatment against oral carcinogenesis at week 26. (B) Incidence of dysplasia and incidence of invasive squamous cell carcinoma by treatment group.

4.2.4. Immunoblot analysis of mechanisms of interaction

The AKT pathway is downstream of the EGFR and has previously been shown to be inhibited by calcitriol (60). We therefore examined the effects of these two agents on the levels of phosphorylated EGFR and AKT immediately following completion of treatment (week 18) and 8 weeks following cessation of treatment (week 26). We also examined the effects of the agents on the vitamin D receptor since the response of cells to calcitriol is dependent on the presence of VDR (**Figure 9, 10**). Although calcitriol and erlotinib did not exhibit significant effects on p-EGFR or p-AKT as single agents, combination treatment caused a modest reduction in p-EGFR at week 18 (**Figure 9B**) and week 26 (**Figure 10B**). Notably, immunoblotting of whole tongue extracts revealed a significant reduction in p-AKT following combination treatment compared to control animals ($p<0.05$) at week 26 (**Figure 10C**). VDR levels were lower among all treatment groups compared to controls at week 18 (**Figure 9D**). At week 26, combination treatment resulted in a significantly lower VDR expression compared to single agent erlotinib (**Figure 10D**).

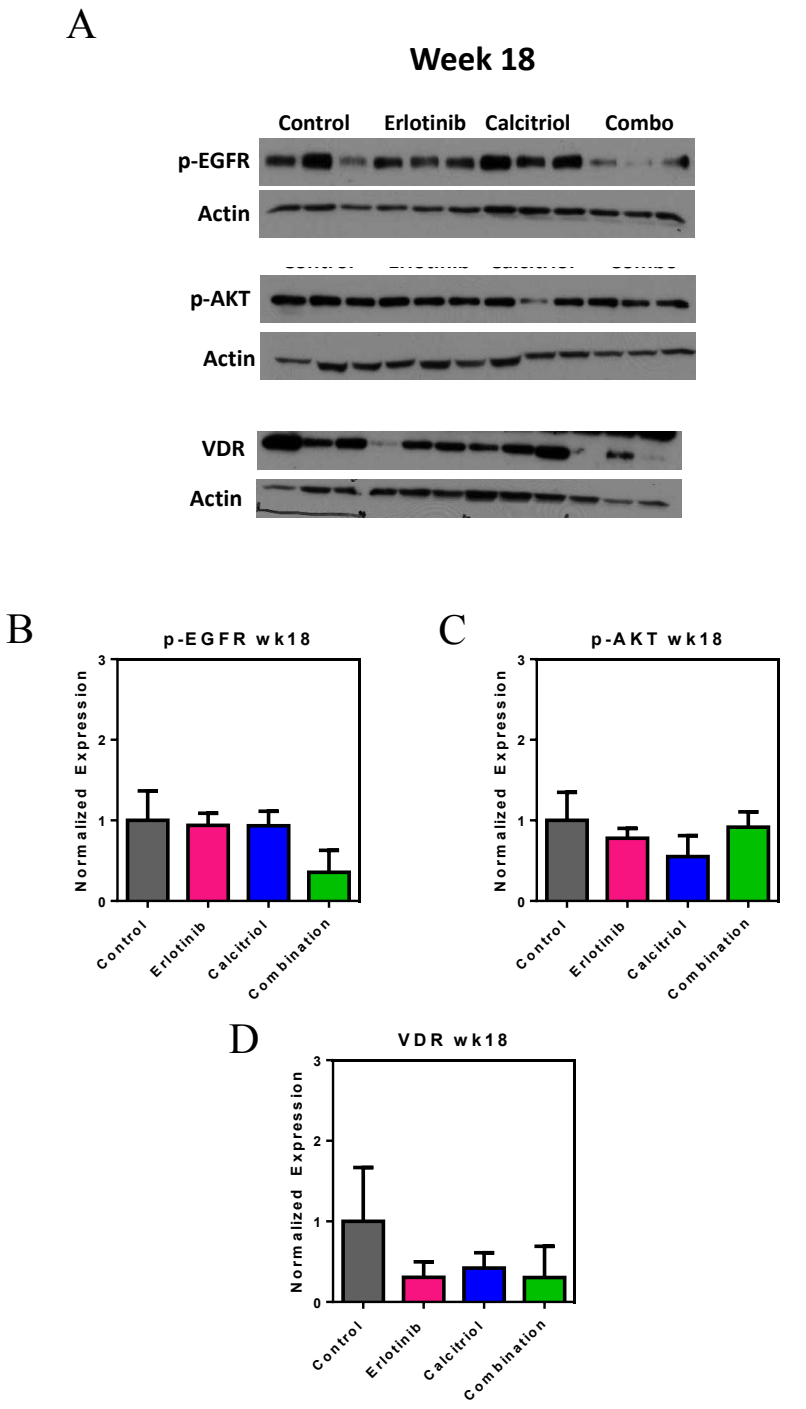

Figure 9. Immunoblot analysis of molecular changes immediately post chemoprevention treatment. (A) Protein expression levels of p-AKT, p-EGFR, and VDR among all groups at week 18 (24 hours post completion of 4-week treatment regime). **(B)** Protein expression levels of p-AKT, p-EGFR, and VDR among all groups at week 18. Whole tongue extracts; n=3 per group ($p<0.05$).

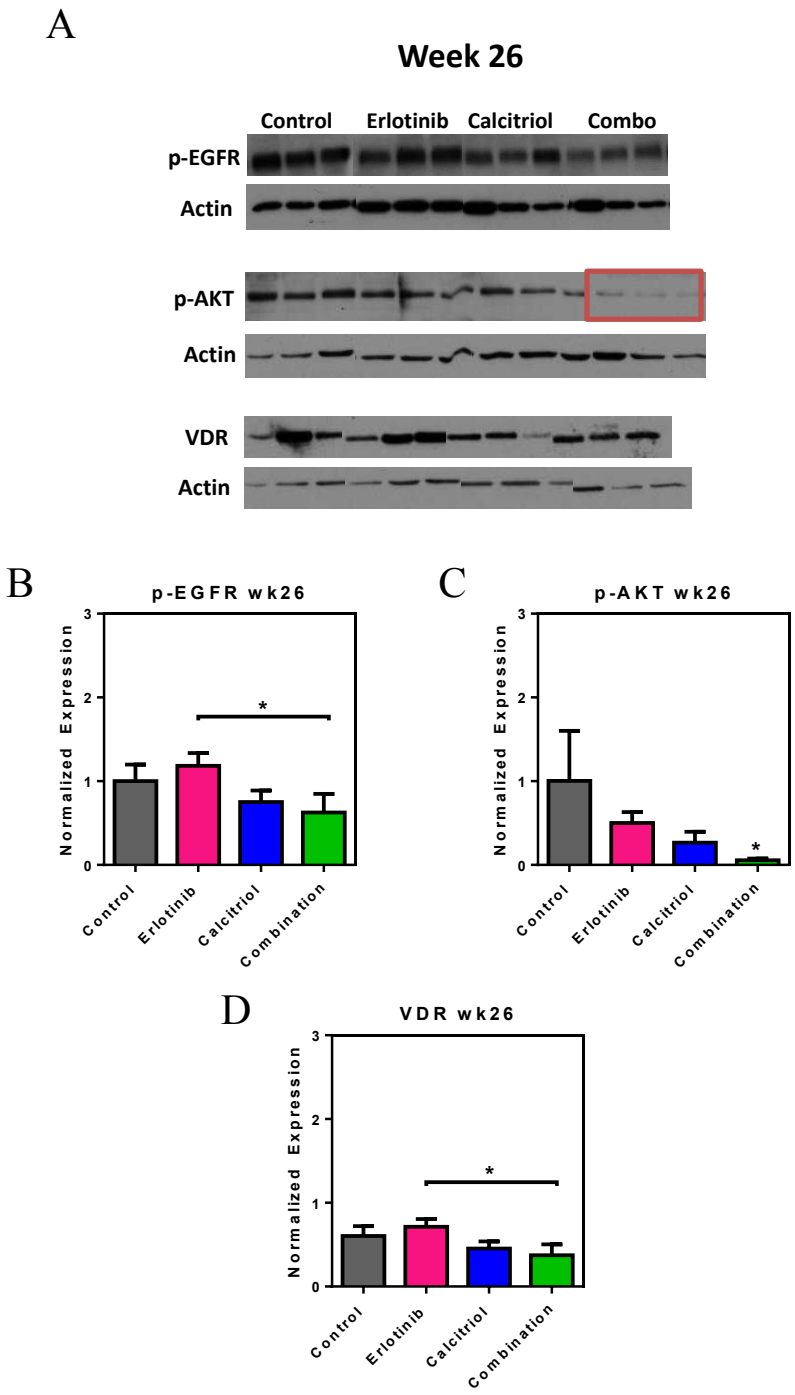

Figure 10. Immunoblot analysis of molecular changes in response to chemoprevention treatment. (A) Protein expression levels of p-AKT, p-EGFR, and VDR among all groups at week 26 (12 weeks post completion of 4-week treatment regime). **(B)** Protein expression levels of p-AKT, p-EGFR, and VDR among all groups at week 26. Whole tongue extracts; n=3 per group ($p<0.05$).

4.2.5. Safety of combined erlotinib-calcitriol treatment

Body weight measurements were obtained throughout the course of the study as a measure of safety and tolerability of the treatments. No significant changes in body weight were seen among any of the groups throughout 4NQO exposure and treatment with erlotinib, calcitriol or combination (**Figure 11A**). Given the potential risk of cardiotoxicity associated with tyrosine kinase inhibitors, we utilized echocardiography to assess cardiac function in animals following treatment. No significant difference in parameters of cardiovascular function (cardiac output, ejection fraction, stroke volume) was observed between animals in control and treatment arms post completion of 4 weeks of treatment (**Figure 11B**).

A

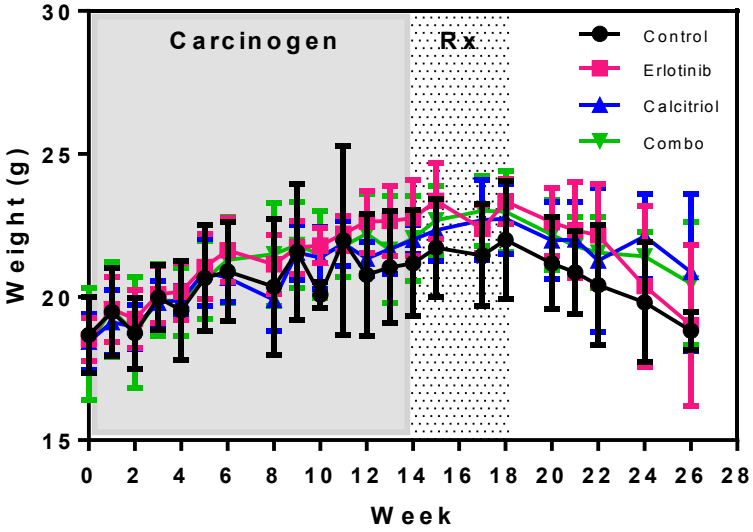

B

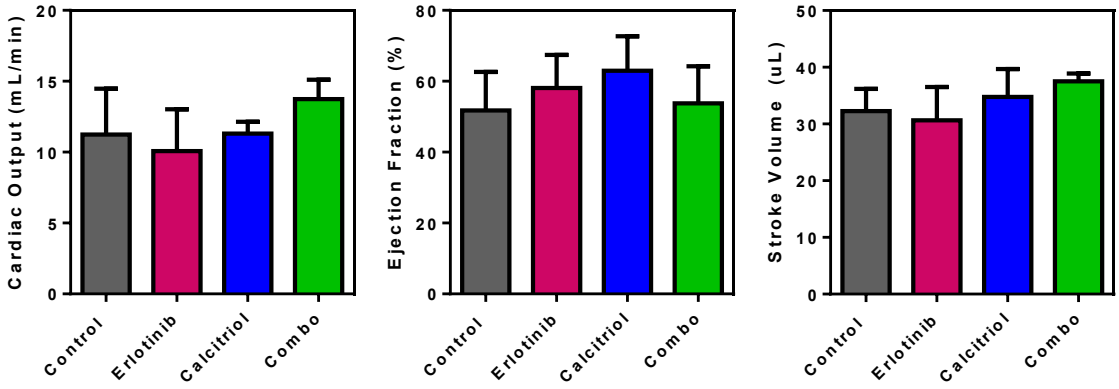

Figure 11. Safety and toxicity assessment. (A) Body weight measurements throughout carcinogen exposure and chemoprevention treatment; n=5 per group. **(B)** Echocardiographic measurement of cardiac output, ejection fraction, and stroke volume at week 21 (3 weeks post completion of erlotinib, calcitriol, or combination treatment); n=3 per group.

CHAPTER 5. DISCUSSION AND FUTURE DIRECTIONS

Head and neck cancers are aggressive tumors most often treated with non-selective therapies. As a result, head and neck patients often experience systemic toxicity, severe treatment-related comorbidities, and poor quality of life post-treatment. In addition, high rate of recurrence and formation of second primary tumors (3, 16, 43) remain prevalent. Given this reality, a more strategic approach to combat head and neck cancer and improve patient quality of life would be to examine novel prevention strategies that can be safely and effectively administered. As previously mentioned, for proper investigation into the effectiveness of a chemoprevention approach, a preclinical model system that mimics the multi-stage progression of human disease is of absolute importance. 4-nitroquinoline-1-oxide administration to rodents forms DNA adducts, causing DNA damage which mimics the damage caused by tobacco smoke in humans (61). The molecular events induced by 4NQO have been shown to mimic the multi-stage progression of human disease, thereby confirming the applicability of this model to our studies (61, 67). Utilization of the 4NQO model of oral carcinogenesis allowed for an effective method to test the impact of calcitriol, the active metabolite of vitamin D, on the chemopreventive efficacy of the EGFR inhibitor, erlotinib, against HNSCC.

To carry out our investigation of this chemoprevention approach, we utilized a non-invasive imaging method. Although cancer is a chronic process, very few studies have utilized longitudinal imaging to monitor the oral carcinogenesis process *in vivo*. The majority of studies have utilized histopathologic evaluation, which will always remain important. However, given the invasive nature of this technique, serial assessment of changes within the same experimental cohort cannot be achieved. Published preclinical work has characterized molecular changes within the 4NQO model at various time points (62, 68). Other preclinical studies in the 4NQO

model have utilized various methods of assessing longitudinal changes associated with the carcinogenesis process, such as nuclear magnetic resonance spectroscopy, autofluorescence, and digital imaging (69, 70). However, to our knowledge, longitudinal imaging studies in the 4NQO model have not been carried out on the same animals over time. To achieve serial assessment of oral carcinogenesis in the 4NQO model, we utilized magnetic resonance imaging. MRI is clinically relevant and offers the ability to non-invasively detect visual and functional changes within the tissue. In particular, we employed T2-weighted MRI, which takes advantage of the intrinsic properties within the tissue to provide contrast among the different tissues being imaged (71). Utilization T2-weighted imaging allowed for assessment of morphologic changes in the tissue without the use of exogenous contrast agents. Based on MRI, we saw suppression of tumor growth and decreased tumor incidence in the combination treatment group. Although these results are encouraging, investigation into longer durations of treatment is warranted to better mimic the clinical setting.

An extensive body of literature exists on the anti-neoplastic activity of calcitriol against breast, prostate, colon and skin cancers (51-53, 57-59). Studies have also reported on the growth inhibitory effects of calcitriol against SCC and oral SCC cell lines (53, 57, 72-74). Meier *et al*. have shown that administration of vitamin D_3 delayed the oral carcinogenesis process in the hamster buccal pouch SCC model (72). At the clinical level, Walsh *et al*. have demonstrated an immunomodulatory effect produced by treatment of vitamin D_3 in patients with HNSCC, which led to overall slower time to recurrence of disease post-surgery compared to untreated patients (75). In addition, combination treatment of vitamin D_3 and erlotinib in acute myeloid leukemia cells has exhibited synergistic anti-proliferative and pro-apoptotic effects (76). We therefore

investigated if calcitriol could enhance the efficacy of an EGFR inhibitor against oral squamous cell carcinoma.

The effects of calcitriol are mediated by its interaction with the vitamin D receptor (49). The VDR is located primarily in the nucleus and binds to vitamin D response elements resulting in activation or repression of target genes. The presence of VDR has been documented in normal tissue types, such as, the intestinal tract, kidneys and bone, as well as in epithelial and mesenchymal tumors including breast, prostate and colon carcinomas and osteosarcomas (49, 50). Several endothelial cell types including murine and bovine aortic endothelial cells and human capillaries also express VDR (58, 77). Given that the effects of calcitriol seem to be conditional upon the expression of VDR in the target tissue (57, 64, 65), we examined the status of VDR expression in our carcinogen-induced mouse model. When comparing an untreated mouse tongue to a tongue exposed to the carcinogen, 4NQO, we found that the intensity of VDR staining was increased in carcinogen-exposed epithelium compared to healthy epithelial tissue. Consistent with our findings, recent published literature has revealed that VDR expression is much higher in both human and murine oral SCC than in normal oral epithelium (78). In normal oral epithelium, VDR expression was found to be predominantly in the basal layer, while in neoplastic lesions, VDR expression was dispersed throughout the epithelium (79).

Published literature of preclinical studies in colon and breast cancer models has demonstrated interactions of vitamin D_3 and the epidermal growth factor on expression of EGFR and VDR, respectively (79-81) However, modulation of EGFR by vitamin D_3 appears to be dependent on the cell type. Conflicting results have been reported in two different breast cancer cell lines; Koga *et al*. found that treatment with vitamin D_3 resulted in a decrease in EGFR number, while Desprez *et al*. found that vitamin D_3 treatment resulted in an increase in EGFR

expression (80, 81). In a human colon adenocarcinoma cell line, treatment with vitamin D_3 resulted in a decreased abundance of EGFR (79). Tong *et al*. also found that the epidermal growth factor suppressed expression of the VDR (79). Furthermore, in an epidermoid carcinoma cell line, treatment with 1,25-D_3 downregulated EGFR-growth signaling and reduced EGF-induced tyrosine phosphorylation of the EGFR (82). The presence of crosstalk between these two intracellular signaling pathways has been documented; however, the extent to which the pathways interact in oral SCC is unknown. To investigate possible interactions between the two agents, we performed western blot analyses on mouse tongue extracts at multiple time points post treatment with erlotinib and calcitriol. As previously stated, immediately post 4 weeks treatment (week 18), expression of p-EGFR in combination-treated tongues was reduced compared to all other groups. At week 26, combination-treated tongues had a significantly lower expression of p-EGFR compared to tongues treated with single agent erlotinib, as well as a significantly lower expression of p-AKT compared to controls. Although the mechanism of interaction between the two agents requires further investigation, these results indicate presence of crosstalk between the two agents resulting in sustained inhibition of multiple signaling pathways downstream of EGFR with the combination treatment.

Prior clinical work has demonstrated the safety and tolerability of both erlotinib and calcitriol as single agents (36, 37, 45, 83-85). Unlike cetuximab, which requires an intravenous injection, erlotinib is orally active and can be taken at the patient's home. As previously mentioned, erlotinib is currently being investigated for its efficacy in chemoprevention and treatment of HNSCC (37, 47). Erlotinib is FDA-approved for treatment in patients with non-small cell lung cancer, as well as treatment in combination with gemcitabine for locally advanced and metastatic pancreatic cancer (86, 87). Clinical dosing of erlotinib typically ranges

from 100 mg to 150 mg daily (86, 87). Most preclinical studies have documented erlotinib's therapeutic efficacy at 50 mg/kg or higher in mice, which corresponds to approximately 240 mg or more daily in humans, much greater than the amount currently given in the clinic (88-90). Our studies have demonstrated tumor growth inhibition in mice at 25 mg/kg daily for 4 weeks. This dose corresponds to approximately 122 mg daily in humans (90). A recent clinical trial investigating daily erlotinib (150 mg) as an adjuvant in head and neck cancer patients who had recently undergone salvage surgery found poor tolerance to long-term treatment at this dose. Of the 31 patients enrolled in the study, only 8 patients completed the 12-month course of erlotinib therapy given at 150 mg, 5 days per week. Discontinuation of treatment as well as dose reductions occurred as a result of intolerance to prolonged therapy (37). Although our studies investigated a lower dose of erlotinib, future studies into even lower doses at longer durations need to be performed to better mimic a chemoprevention clinical trial. In addition, clinical trials have exhibited the safety and tolerability of calcitriol administration (83-85). In our study, calcitriol was administered to mice at a dose of 0.1 μg (i.p) 3 days/week (MWF) for 4 weeks. This dosing in an SCC animal model has previously exhibited therapeutic efficacy (91). Daily administration of calcitriol has been shown to be associated with risk of hypercalcemia (92). However, intermittent dosing has exhibited therapeutic efficacy in addition to decreased risk of toxicity-related side effects (83, 84, 93). While no evidence of toxicity was observed with both agents at the doses evaluated in our studies, future studies should therefore investigate the efficacy and toxicity of long-term treatment at multiple doses and schedules.

We recognize the limitations of our study. Although we have shown promising results in our combination regimen, we observed that single agent calcitriol treatment had possible growth stimulatory effects as demonstrated by the higher mean tumor volume compared to the control

group detected through MRI. Prior *in vitro* studies have shown that calcitriol has growth stimulatory effects on the nontumorigenic oral cell line, HGF-1, in a dose-dependent manner (74). In addition, studies examining oral keratinocytes have found that vitamin D_3 treatment stimulates proliferation, most likely due to up-regulation of proteins belonging to the ErbB family or tyrosine kinase receptors, such as EGFR (94). Whether these findings play a role in growth stimulation of cells in the oral cavity after exposure to carcinogen is not fully known, however, timing of intervention with calcitriol as a preventive agent needs to be investigated further. In this regard, non-invasive imaging techniques can provide useful information on the sequence and timing of application of preventive intervention. Furthermore, clinical translation of effective doses of calcitriol without the risk of hypercalcemia is difficult. Alternative approaches to safely promote local tissue production of 1,25-$(OH)_2D_3$ are warranted. Dietary supplementation of vitamin D has been studied in other preclinical tumor models and in the clinic (95-97). A randomized clinical trial investigating calcium plus vitamin D supplementation in postmenopausal women found a reduced cancer incidence among the combination arm compared to the placebo and calcium-only arms (97). The ease of dietary supplementation makes this approach particularly attractive for clinical translation. To this end, ongoing studies in our laboratory are investigating the effects of dietary vitamin D_3 on the chemoprevention of HNSCC. Further testing of this bio-adjuvant combination chemoprevention approach is required to fully examine its impact throughout the process of oral carcinogenesis.

Literature Cited

1. Forastiere A, Koch W, Trotti A, Sidransky D. Head and Neck Cancer. N Engl J Med 2001; 345: 1890-1900.

2. Melrose RJ. Premalignant oral mucosal diseases. J Calif Dent Assoc 2001; 29:593-600.

3. Leemans CR, Braakhuis BJ, Brakenhoff RH. The molecular biology of head and neck cancer. Nature Rev Cancer 2011; 11:9-22.

4. http://www.cancer.gov/cancertopics/factsheet/Sites-Types/head-and-neck

5. Castellsague X, Quintana MJ, Martinez MC, et al. The role of type of tobacco and type of alcoholic beverage in oral carcinogenesis. Int J Cancer 2004; 108: 741–749.

6. Worsham M, Ali H, Dragovic J, Schweitzer VP. Molecular characterization of head and neck cancer: how close to personalized targeted therapy? Mol Diagn Ther 2012; 16(4): 209-222.

7. Carvalho AL, Nishimoto IN, Califano JA, Kowalski LP. Trends in incidence and prognosis for head and neck cancer in the United States: a site-specific analysis of the SEER database. Int J Cancer. 2005; 114(5): 806–16.

8. Haddad RI, Shin DM. Recent advances in head and neck cancer. N Engl J Med. 2008; 359(11): 1143–54. [PubMed: 18784104].

9. Fung C, Grandis JR. Emerging drugs to treat squamous cell carcinomas of the head and neck. Expert Opin Emerg Drugs 2010; 15(3): 355-373.

10. Ono M, Kuwano M. Molecular mechanisms of epidermal growth factor receptor (EGFR) activation and response to gefitinib and other EGFR-targeting drugs. Clin Cancer Res 2006; 12(24): 7242-7251.

11. Ciardiello F, Tortora G. EGFR antagonists in cancer treatment. N Engl J Med 2008; 358: 1160-1174.

12. Bonner JA, Harari PM, Giralt J, Azarnia N, Shin DM, Cohen RB, et al. Radiotherapy plus cetuximab for squamous-cell carcinoma of the head and neck. N Engl J Med 2006; 354: 567-78.

13. Vermorken JB, Trigo J, Hitt R, Koralewski P, Diaz-Rubio E, Rolland F, et al. Open-label, uncontrolled multicenter phase II study to evaluate the efficacy and toxicity of cetuximab as a single agent in patients with recurrent and/or metastatic squamous cell carcinoma of the head and neck who failed to respond to platinum-based therapy. J Clin Oncol 2007; 25(16): 2171-77.

14. Zimmerman M, Zouhair A, Azria D, Ozsahin M. The epidermal growth factor receptor (EGFR) in head and neck cancer: its role and treatment implications. Radiation Oncology 2006; 1:11.

15. Roskoski R Jr. The ErbB/HER receptor protein-tyrosine kinases and cancer. Biochem Biophys Res Comm 2004; 319: 1-11.

16. Grandis JR, Tweardy DJ. Elevated levels of transforming growth factor alpha and epidermal growth factor receptor messenger RNA are early markers of carcinogenesis in head and neck cancer. Cancer Res 1993; 53(15): 3579-84.

17. Mukaida H, Toi. M, Mirai. T, Yamashita Y, Toge T. Clinical significance of the expression of epidermal growth factor and its receptor in esophageal cancer. Cancer 1991; 68: 142-148.

18. Gupta AK, McKenna WG, Weber CN, et al: Local recurrence in head and neck cancer: Relationship to radiation resistance and signal transduction. Clin Cancer Res 2002; 8: 885-892.

19. Ang KK, Berkey BA, Tu X, et al: Impact of epidermal growth factor receptor expression on survival and pattern of relapse in patients with advanced head and neck carcinoma. Cancer Res 2002; 62: 7350-7356.

20. Rubin Grandis J, Melhem MF, Gooding WE, et al: Levels of TGF-alpha and EGFR protein in head and neck squamous cell carcinoma and patient survival. J Natl Cancer Inst 1998; 90: 824-832.

21. Pomerantz RG and Grandis JR. The epidermal growth factor receptor signaling network in head and neck carcinogenesis and implications for targeted therapy. Semin Oncol 2004; 31: 734–743

22. Soulieres D, Senzer NN, Vokes EE, Hidalgo M, Agarwala SS, Siu LL. Multicenter phase II study of erlotinib, an oral epidermal growth factor receptor tyrosine kinase inhibitor, in patients with recurrent or metastatic squamous cell cancer of the head and neck. J Clin Oncol 2004; 22(1): 77-85.

23. Sporn MB, Suh N. Chemoprevention of cancer. Carcinogenesis 2000; 21(3): 525-530.

24. Steward WP, Brown K. Cancer chemoprevention: a rapidly evolving field. British J Cancer 2013; 109: 1-7.

25. Fisher B, Constantino JP, Wickerham L, Redmond CK, Kavanah M, Cronin WM, Vogel V, Robidoux A, Dimitrov N, Atkins J, Daly M, Wieand S, Tan-Chiu E, Ford L, Wolmark N. Tamoxifen for prevention of breast cancer: report of the national surgical adjuvant breast and bowel project P-1 study. J Natl Cancer Inst 1998; 90(18): 1371-1388.

26. B. Fisher, J.P. Costantino, D.L. Wickerham, R.S. Cecchini, W.M. Cronin, A. Robidoux, T.B. Bevers, M.T. Kavanah, J. Atkins, R.G. Margolese, C.D. Runowicz, J.M. James, L. G. Ford, N. Wolmark. Tamoxifen for prevention of breast cancer: current status of the national surgical adjuvant breast and bowel project P-1 study. J Natl Cancer Inst 2005; 97 (22).

27. G. Steinbach, P. M. Lynch, R. K. S. Phillips et al. The effect of celecoxib, a cyclooxygenase-2 inhibitor, in familial adenomatous polyposis. N Engl J Med 2000; 342 (26): 1946–52.

28. Shin DM, Charuruks N, Lippman SM, Lee JJ, Ro JY, Hong WK, et al. p53 protein accumulation and genomic instability in head and neck multistep tumorigenesis. Cancer Epidemiol Biomarkers Prev 2001; 10(6): 603–9.

29. Park BJ, Chiosea SI, Grandis JR. Molecular changes in the multistage pathogenesis of head and neck cancer. Cancer Biomark 2010; 9(1–6): 325–39.

30. Saba NF, Haigentz M, Vermorken JB, Strojan P, Bossi P, Rinaldo A, Takes RP, Ferlito A. Prevention of head and neck squamous cell carcinoma: removing the "chemo" from chemoprevention. Oral Onc 2014. [Epub ahead of print]

31. Stich HF, Hornby AP, Mathew B, Sankaranarayanan R, Nair MK. Response of oral leukoplakias to the administration of vitamin A. Cancer Lett 1988; 40(1): 93–101.

32. Hong WK, Endicott J, Itri LM, Doos W, Batsakis JG, Bell R, et al. 13-Cis-retinoic acid in the treatment of oral leukoplakia. N Engl J Med 1986; 315(24): 1501–5.

33. Lippman SM, Batsakis JG, Toth BB, Weber RS, Lee JJ, Martin JW, et al. Comparison of low-dose isotretinoin with beta carotene to prevent oral carcinogenesis. N Engl J Med 1993; 328(1): 15–20.

34. Hong WK, Lippman SM, Itri LM, Karp DD, Lee JS, Byers RM, et al. Prevention of second primary tumors with isotretinoin in squamous-cell carcinoma of the head and neck. N Engl J Med 1990; 323(12): 795–801.

35. Smith W, Saba NF. Retinoids as chemoprevention for head and neck cancer: where do we go from here? Crit Rev Oncol Hematol 2005; 55(2): 143–52.

36. William NW, Papadimitrakopoulou V, Lee JJ, Mao L, Lin H, Gillenwater AM, et al. Randomized placebo-controlled trial (RCT) of erlotinib for prevention of oral cancer (EPOC). J Clin Oncol 2014; 32: 5s. Abstract 6007.

37. Rosenthal EL, Chung TK, Carroll WR, Clemons L, Desmond R, Nabell L. Assessment of erlotinib as adjuvant chemoprevention in high-risk head and neck cancer patients. Ann Surg Oncol 2014; 21(13): 4263–9.

38. Papadimitrakopoulou VA, William Jr WN, Dannenberg AJ, Lippman SM, Lee JJ, Ondrey FG, et al. Pilot randomized phase II study of celecoxib in oral premalignant lesions. Clin Cancer Res 2008; 14(7): 2095–101.

39. Chen Z, Zhang X, Li M, Wang Z, Wieand HS, Grandis JR, et al. Simultaneously targeting epidermal growth factor receptor tyrosine kinase and cyclooxygenase-2, an efficient approach to inhibition of squamous cell carcinoma of the head and neck. Clin Cancer Res 2004; 10(17): 5930–9.

40. Zhang X, Chen ZG, Choe MS, Lin Y, Sun SY, Wieand HS, et al. Tumor growth inhibition by simultaneously blocking epidermal growth factor receptor and cyclooxygenase-2 in a xenograft model. Clin Cancer Res 2005; 11(17): 6261–9.

41. Choe MS, Zhang X, Shin HJ, Shin DM, Chen ZG. Interaction between epidermal growth factor receptor- and cyclooxygenase 2-mediated pathways and its implications for the chemoprevention of head and neck cancer. Mol Cancer Ther 2005; 4(9): 1448–55.

42. Grandis JR, Sok JC. Signaling through the epidermal growth factor receptor during the development of malignancy. Pharmacol Ther 2004; 102(1): 37-46.

43. Taoudi Benchekroun M, Saintigny P, Thomas SM, El-Naggar AK, Papadimitrakopoulou V, Ren H, et al. Epidermal growth factor receptor expression and gene copy number in the risk of oral cancer. Cancer Prev Res 2010; 3(7): 800-809.

44. Saba NF, Hammond A, Shin DM, Khuri FR. Moving toward bioadjuvant approaches to head and neck cancer prevention. Int J Radiat Oncol Biol Phys 2007; 69(2 Suppl): S132-35.

45. Saba NF, Hurwitz SJ, Kono S, Yang CS, Zhao Y, Chen Z, et al. Chemoprevention of head and neck cancer with celecoxib and erlotinib: results of a phase Ib and pharmacokinetic study. Cancer Prev Res 2014; 7(3): 283-91.

46. National Cancer Institute; Sidney Kimmel Comprehensive Cancer Center. Cetuximab in Treating Patients With Precancerous Lesions of the Upper Aerodigestive Tract. In: ClinicalTrials.gov [Internet]. Bethesda (MD): National Library of Medicine (US). 2012- [cited 2014 Oct 20]. Available from: http://clinicaltrials.gov/show/ NCT00524017 NLM Identifier: NCT00524017.

47. Astellas Pharma Inc, Polyphenon Pharma; Emory University. Phase I Chemoprevention Trial With Green Tea Polyphenon E and Erlotinib in Patients With Premalignant Lesions of the Head and Neck. In: ClinicalTrials.gov [Internet]. National Library of Medicine (US). 2014- [cited 2014 Oct 20]. Available from: http://clinicaltrials.gov/show/ NCT01116336 NCT Identifier: NCT01116336.

48. Zhang X, Zhang H, Tighiouart M, Lee JE, Shin HJ, Khuri FR, et al. Synergistic inhibition of head and neck tumor growth by green tea (2)-epigallocatechin-3-gallate and EGFR tyrosine kinase inhibitor. Int J Cancer 2008; 123: 1005-14.

49. Bikle DD, Pillai S. Vitamin D, calcium, and epidermal differentiation. Endocrine Rev 1993; 14: 3-19.

50. Reichekl H, Koeffler HP, Norman AW. The role of the vitamin D endocrine system in health and disease. New Engl J Med 1989; 320(15): 980-91.

51. Weinstein SJ, Purdue MP, Smith-Warner SA, Mondul AM, Black A, Ahn J,et al. Serum 25-hydroxyvitamin D, vitamin D binding protein and risk of colorectal cancer in the Prostate, Lung, Colorectal and Ovarian Cancer Screening Trial. Int J Cancer 2014.[Epub ahead of print]

52. Leyssens C, Verlinden L, Verstuyf A. Antineoplastic effects of $1,25(OH)_2D_3$ and its analogs in breast, prostate and colorectal cancer. EndocrRelat Cancer 2013; 20(2): R31-47.

53. McElwain MC, Dettlebach MA, Modezelewski RA, et al. Antiproliferative effects in vitro and in vivo of 1,25-dihydroxyvitamin D3 and a vitamin D3 analog in a squamous cell carcinoma model system Mol Cell Diff 1995; 3: 31-50.

54. Flanagan JN, Young MV, Persons KS, Wang L, Mathieu JS, Whitlatch LW, Holick MF, Chen TC. Vitamin D metabolism in human prostate cells: implications for prostate cancer chemoprevention by vitamin D. Anticancer Res 2006; 26: 2567-2572.

55. Fleet JC. Molecular actions of vitamin D contributing to cancer prevention. Mol Aspects Med 2008; 29: 388-396.

56. Guraya SY. Chemopreventive role of vitamin D in colorectal carcinoma. J Microscopy and Ultrastructure 2014; 2: 1-6.

57. Johnson CS, Muindi JR, Hershberger PA, Trump DL. The antitumor efficacy of calcitriol: preclinical studies. Anticancer Res 2006; 26(4A): 2543-49.

58. Bernardi RJ, Johnson CS, Modzelewski RA, Trump DL. Antiproliferative effects of 1α,25-dihydroxyvitamin D(3) and vitamin D analogs on tumor-derived endothelial cells. Endocrinology 2002; 143: 2508-14.

59. Freudlsperger C, Burnett JR, Friedman JA, Kannabiran VR, Chen Z, Van Waes C. EGFR-PI3K-AKT-mTOR signaling in head and neck squamous cell carcinomas: attractive targets for molecular-oriented therapy. Expert Opin Ther Targets 2011; 15(1): 63-74.

60. McGuire TF, Trump DL, Johnson CS Vitamin D(3)-induced apoptosis of murine squamous cell carcinoma cells. Selective induction of caspase-dependent MEK cleavage and up-regulation of MEKK-1. J Biol Chem 2001; 276: 26365–73.

61. Kanojia D, Vaidya MM. 4-nitroquinoline-1-oxide induced experimental oral carcinogenesis. Oral Oncology 2006; 42: 655-67.

62. Vitale-Cross L, Molinolo AA, Marin D, et al. Metformin prevents the development of oral squamous cell carcinomas from carcinogen-induced premalignant lesions. Cancer Prev Res 2012; 5: 562-73.

63. Jayaprakash V, Sullivan M, Merzianu M, Rigual NR, Loree TR, Popat SR, et al. Autofluorescence-guided surveillance for oral cancer. Cancer Prev Res 2009; 2(11): 966-74.

64. Stumpf WE, Sar M, Reid FA, Tanaka Y, DeLuca HF. Target cells for 1,25-dihydroxyvitamin D3 in intestinal tract, stomach, kidney, skin, pituitary, and parathyroid. Science 1979; 206: 1188–90.

65. Menezes RJ, Cheney RT, Husain A, Tretiakova M, Loewen G, Johnson CS, et al. Vitamin D receptor expression in normal, premalignant, and malignant human lung tissue. Cancer Epidemiol Biomarkers Prev 2008; 17(5): 1104-10.

66. Segaert S, Degreef H, Bouillon R. Vitamin D Receptor Expression Is Linked to Cell Cycle Control in Normal Human Keratinocytes. Biochem and Biophys Res Comm 2000; 279: 89-94.

67. Wong KK. Oral-specific chemical carcinogenesis in mice: an exciting model for cancer prevention and therapy. Cancer Prev Res 2009; 2(1): 10-13.

68. Czeminski R, Amomphimoltham P, Patel V, Molinolo AA, Gutkind JS. Targeting mammalian target of rapamycin by rapamycin prevents tumor progression in an oral-specific chemical carcinogensis model. Canc Prev Res 2009; 2(1): 27-36.

69. Kong X, Yang X, Zhou J, Chen S, Li X, Jian F, Deng P, Li W. Analysis of plasma metabolic biomarkers in the development of 4-nitroquinoline-1-oxide-induced oral carcinogenesis in rats. Oncol Lett 2015; 9(1): 283-289.

70. Hellebust A, Rosbach K, Wu JK, Nguyen J, Gillenwater A, Vigneswaran N, Richards-Kortum R. Vital-dye-enhacned multimodal imaging of neoplastic progression in a mouse model of oral carcinogenesis. J Biomed Opt 2013; 18(12): 126017.

71. Mitchell DG, Burk DL, Vinitski S, Rifkin MD. The biophysical basis of tissue contrast in extracranial MR imaging. Am J Roentgenol 1987; 149(4): 831-837.

72. Meier JD, Enepekides DJ, Poirier B, Bradley CA, Albala JS, Farwell G. Treatment with 1-alpha,25-dihydroxyvitamin D_3 (vitamin D_3) to inhibit carcinogenesis in the hamster buccal pouch model. Arch Otolaryngol Head Neck Surg 2007; 133(11): 1149-52.

73. Chiang KC, Yeh CN, Hsu JT, Chen LW, Kuo SF, Sun CC, et al. MART-10, a novel vitamin D analog, inhibits head and neck squamous carcinoma cells growth through cell cycle arrest at G_0/G_1 with upregulation of p21 and p27 and downregulation of telomerase. J Steroid Biochem Mol Biol 2013; 138: 427-34.

74. Osafi J, Hejazi A, Stutz DD, Keiserman MA, Bergman CJ, Kingsley K. Differential effects of 1,25-dihydroxyvitamin D_3 on oral squamous cell carcinomas in vitro. J Dietary Suppl 2014; 11: 145-54.

75. Walsh JE, Clark AM, Day TA, Gillespie MB, Young MRI. Use of α,25-dihydroxyvitamin D_3 treatment to stimulate immune infiltration into head and neck squamous cell carcinoma. Hum Immunol 2010; 71: 659-65.

76. Lainey E, Wolfromm A, Sukkurwala AQ, Micol JB, Fenaux P, Galluzzi L, et al. EGFR inhibitors exacerbate differentiation and cell cycle arrest induced by retinoic acid and vitamin D_3 in acute myeloid leukemia cells. Cell Cycle 2013; 12: 2978-2991.

77. Merke J, Milde P, Lewicka S, Hügel U, Klaus G, Mangelsdorf DJ, et al. Identification and regulation of 1,25-dihydroxyvitamin D_3 receptor activity and biosynthesis of 1,25-dihydroxyvitamin D_3. Studies in cultured bovine aortic endothelial cells and human dermal capillaries. J Clin Invest 1989; 83: 1903-15.

78. Yuan FN, Valiyaparambil J, Woods MC, Tran H, Pant R, Adams JS, et al. Vitamin D signaling regulates oral keratinocyte proliferation *in vitro* and *in vivo*. Int J Oncol 2014; 44(5): 1625–33.

79. Tong WM, Kállay E, Hofer H, Hulla W, Manhardt T, Peterlik M, et al. Growth regulation of human colon cancer cells by epidermal growth factor and 1,25-dihydroxyvitamin D3 is mediated by mutual modulation of receptor expression. Eur J Cancer 1998; 34: 2119-25.

80. Koga M, Eisman JA, Sutherland RL. Regulation of epidermal growth factor receptor levels by 1,25-dihydroxyvitamin D_3 in human breast cancer cells. Cancer Res 1988; 48: 2734-39.

81. Desprez PY, Poujol D, Falette N, Lefebvre MF, Saez S. 1,25-dihydroxyvitamin D3 increase epidermal growth factor receptor gene expression in BT-20 breast carcinoma cells. Biochem Biophys Res Commun 1991; 176: 1-6.

82. Cordero JB, Cozzolino M, Lu Y, Vidal M, Slatopolsky E, Stahl PD, et al. 1,25-dihydroxyvitamin D down-regulates cell membrane growth- and nuclear growth-promoting signals by the epidermal growth factor receptor. J Biol Chem 2002; 277: 38965-71.

83. Smith DC, Johnson CS, Freeman CC, Muindi J, Wilson JW, Trump DL. A phase I trial of subcutaneous calcitriol (1,25-dihydroxycholecalciferol) in patients with advanced malignancy. Clin Cancer Res 1999; 5: 1339-45.

84. Beer TM, Munar M, Henner WB. A phase I trial of pulse calcitriol in patients with refractory malignancies. Cancer 2001; 91(12): 2431-39.

85. Fakih MG, Trump DL, Muindi JR, Black JD, Bernardi RJ, Creaven PJ, et al. A phase I pharmacokinetic and pharmacodynamic study of intravenous calcitriol in combination with oral gefitinib in patients with advanced solid tumors. Clin Cancer Res 2007; 13(4): 1216-23.

86. Cohen MH, Johnson JR, Chen YF, Sridhara R, Pazdur R. FDA drug approval summary: erlotinib (Tarceva) tablets. The Oncologist 2005; 10(7): 461-466.

87. Moore MJ, Goldstein D, Hamm J, Figer A, Hecht JR, Gallinger S, Au HJ, et al. Erlotinib plus gemcitabine compared with gemcitabine alone in patients with advanced pancreatic cancer: a phase III trial of the National Cancer Institute of Canada Clinical Trials Group. J Clin Oncol 2007; 25(15): 1960-6.

88. Cassell A, Freilino ML, Lee J, Barr S, Wang L, Panahandeh MC, et al. Targeting TORC1/2 enhances sensitivity to EGFR inhibitors in head and neck cancer preclinical models. Neoplasia 2012; 14(11): 1005-14.

89. Shin DM, Zhang H, Saba NF, Chen AY, Nannapaneni S, Amin AR, et al. Chemoprevention of head and neck cancer by simultaneous blocking of epidermal growth factor receptor and cyclooxygenase-2 signaling pathways: preclinical and clinical studies. Clin Cancer Res 2013; 19(5): 1244-56.

90. Reagan-Shaw S, Nihal M, Ahmad N. Dose translation from animal to human studies revisted. FASEB J 2008; 22(3): 659-61.

91. Bernardi R, Johnson CJ, Trump DL. ZD1839 (Iressa), a selective epidermal growth factor receptor tyrosine kinase inhibitor (EGFR-TKI), enhances the antiproliferative effects of calcitriol(1,25-dihydroxyvitamin D3) in squamous cell carcinoma: effects on ERK and Akt [abstract 3883] Proc Am Assoc Cancer Res 2007; 13: 1216-1223.

92. Osborn JL, Schwartz GG, Smith DC, Bahnson R, Day R, Trump DL. Phase II trial of oral 1,25-dihydroxyvitamin D (calcitriol) in hormone refractory prostate cancer. Urolog Oncol: Seminars and Original Investigations 1995; 1(5): 195-198.

93. Beer TM, Eilers KM, Garzotta M, Egorin MJ, Lowe BA, Henner WD. Weekly high-dose calcitriol and docetaxel in metastatic androgen-independent prostate cancer. J Clin Oncol 2003; 21: 123-128.

94. Garach-Jehoshua O, Ravid A, Liberman UA, Koren R. 1,25-dihydroxyvitamin D3 increases the growth-promoting activity of autocrine epidermal growth factor receptor ligands in keratinocytes. Endocrinology 1999; 140: 713-21.

95. Krishnan AV, Swami S, Feldman D. Equivalent anticancer activities of dietary vitamin D and calcitriol in an animal model of breast cancer: importance of mammary CYP27B1 for treatment and prevention. J Steroid Biochem Mol Biol 2013; 136: 289-295.

96. Meeker S, Seamons A, Paik J, et al. Increased dietary vitamin D suppresses MAPK singaling, colitis, and colon cancer. Cancer Res 2014; 74: 4398-4408.

97. Sperati F, Vici P, Maurgeri-Saccà M, Stranges S, Santesso N, Mariani L, et al. Vitamin D supplementation and breast cancer prevention: A systematic review and meta-analysis of randomized clinical trials. Plos One 2013; 8(7): 1-9.